Science of the Total Environment 789 (2021) 147909

Contents lists available at ScienceDirect

Science of the Total Environment

journal homepage: www.elsevier.com/locate/scitotenv

The origin of the saline waters in the Villafáfila lakes (NW Spain). A hydrogeological, hydrochemical, and geophysical approach

Pedro Huerta [a,*], Ildefonso Armenteros [b], Clemente Recio [b], Pedro Carrasco-García [c], Carolina Rueda-Gualdrón [b], Azahara Cidón-Trigo [b]

[a] Dpto. Geología, Escuela Politécnica Superior de Ávila. Universidad de Salamanca, Av. Hornos Caleros, n° 50, 05003 Ávila, Spain
[b] Dpto. Geología, Facultad de Ciencias, Universidad de Salamanca, Pza. de la Merced S/N, 37008 Salamanca, Spain
[c] Dpto. Ingeniería Cartográfica y del Terreno, Escuela Politécnica Superior de Ávila. Universidad de Salamanca, Av. Hornos Caleros, n° 50, 05003 Ávila, Spain

HIGHLIGHTS

- Villafáfila lakes behaves as through flow lakes draining to the Salado river.
- Villafáfila lake waters have meteoric origin, solutes comes from groundwaters
- Basement elevation produces discharge of regional groundwaters
- The main source of solutes are Triassic and Cenozoic evaporites.
- The brine in the lake sediment's aquitard overlies less saline groundwaters

GRAPHICAL ABSTRACT

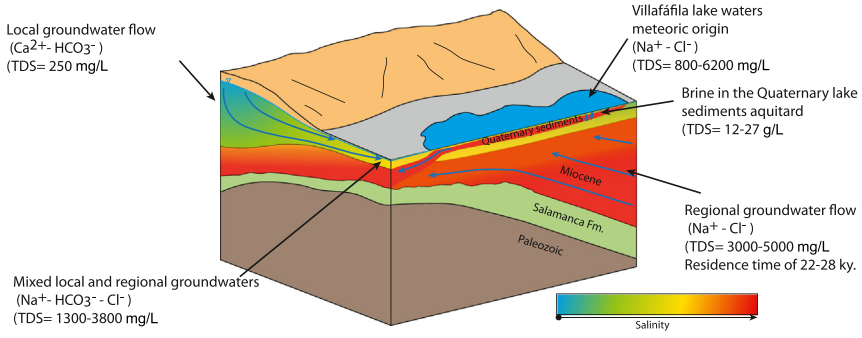

ARTICLE INFO

Article history:
Received 25 February 2021
Received in revised form 14 May 2021
Accepted 16 May 2021
Available online 26 May 2021

Editor: Christian Herrera

Keywords:
Saline lake
Through-flow lake
Regional discharge
Duero hydrological basin
Solute origin
Time domain electromagnetism

ABSTRACT

Villafáfila lakes are a natural reserve included in the intergovernmental RAMSAR agreements for conservation of wetlands, with special interest for their brackish-saline waters. These lakes are located at the western margin of the Duero basin, whose aquifer system has no evaporitic rocks upstream. Understanding the origin of the lake's salinity, the groundwater circulation and the distribution of the brackish-saline waters in the area is important not only for the preservation and management of the natural reserve, but for human water consumption as well. Three types of waters have been identified according to their chemical composition. Type 1 are calcium-bicarbonate fresh waters identified in the local recharge areas (surrounding hills); Type 2 are mixed waters dominated by sodium and chloride-bicarbonate, identified at the toe of the hills; Type 3 are brackish to saline sodium-chloride waters from the lakes, springs and boreholes. Time domain electromagnetic (TDEM) profiles have revealed the existence of a basement elevation that forces brackish regional groundwater flow to rise. Radiocarbon age of regional groundwaters points to residence times of 20–30 Ky. Villafáfila lakes are through-flow lakes nourished by meteoric waters (direct precipitation and shallow groundwaters) as deduced by stable isotopes ($\delta^{18}O_{H2O}$, δD_{H2O}), while the solutes are provided by ascendant deep groundwater flows in the lakes bottom and in the surrounding area. Sulphate stable isotopes ($\delta^{18}O_{SO4=}$; $\delta^{34}S_{SO4=}$) suggest that deep groundwaters have been in contact with Triassic and Cenozoic evaporites. Below the lake's bottom there is a brine (TDS = 27 g/L) contained within the lake-sediment aquitard that is concentrated by evaporation in the vadose zone and by salt recycling. A salinity inversion has been observed below the brine. The lack of saline crusts on the lake's bottom is favored by the SW outflow of the brine.

* Corresponding author.
E-mail address: phuerta@usal.es (P. Huerta).

https://doi.org/10.1016/j.scitotenv.2021.147909
0048-9697/

1. Introduction

Brackish or saline lakes usually occur under arid or semiarid climates where evaporation exceeds precipitations (Hardie et al., 1978). The salinity of lakes, not related to marine waters, commonly originates in areas with salt-bearing rocks in their surroundings (Kohfahl et al., 2008), or is concentrated from runoff and/or groundwaters that have not had contact with highly soluble rocks. In this second case low salinity waters can concentrate by direct evaporation of lake waters in terminal lakes (Jones et al., 2009) or could be previously concentrated in groundwaters. Increasing salinity of groundwaters can be produced by several factors like the residence time of groundwaters in the aquifer, climate change and, in coastal aquifers, sea water intrusion (Bahir et al., 2018; Jacobson et al., 1988; Jones et al., 1977; Ouhamdouch et al., 2019), the interaction with earth's surface (Cartwright et al., 2004, 2009), or the nature of the geological formations, amongst others (Chebotarev, 1955). Long path saline regional flows discharge into rivers, coastal areas, or -in endorheic hydrological basins- large saline lakes. Saline deep waters could be forced to flow up in mid-path areas, upstream the main discharge zones, due to the occurrence of faults or other obstacles in the regional groundwater flow (De la Hera-Portillo et al., 2021) and, if this is the case, saline or brackish water throughflow lakes can occur. In the Duero river hydrological basin, in the western part of the Cenozoic Duero basin, Villafáfila lakes could be an example of this situation. Lithology of the area is sedimentary siliciclastic rocks, mainly sandstones, conglomerates, and mudstones, but Villafáfila lake waters are brackish to saline, and halite-bearing efflorescences occur during the dry season. There are many sources of ions in continental saline lakes (Yechieli and Wood, 2002) but at Villafáfila the brackish deep groundwaters could be the main ion source. The objectives of this research are: i) understanding the groundwater flow patterns and explaining the origin of brackish to saline groundwaters in the area ii) identifying the ion source(s) for lake and groundwaters, and iii) to identify the lake-groundwater interaction. To accomplish these objectives it is important to characterize the basin geology, the lake hydrology, and the hydrochemistry of lake waters and both shallow and deep groundwaters (Bahir et al., 2018; Marazuela et al., 2018; Saeed et al., 2021). Comparative analysis of water chemistry in lakes and associated groundwater flow systems has proven to be a good indicator of these interactions (Cui and Li, 2014; Donovan and Rose, 1994). Stable isotope ratios are a useful tool for understanding lake-groundwater interaction and can help to decipher the origin of different waters and the processes involved (Cartwright et al., 2009; Robinson and Gunatilaka, 1991; Wassenaar et al., 2011). The use of electric geophysics (time-domain electromagnetic surveys; TDEM) can help to reveal not only the aquifer geometry and characteristics (Flores Avilés et al., 2020; Young et al., 1998), but the changes in groundwater salinity as well (Goldman et al., 2004; Levi et al., 2008; Tchouta et al., 2019). The low density of piezometers in the area makes it difficult to measure the hydraulic heads and the scarcity of hydrogeological studies makes this research useful not only for understanding the hydrogeology of the Villafáfila lakes but the dynamics of groundwater discharge in the western part of the Duero basin as well.

These lakes were of economic importance in the area from the Bronze age until the Middle Ages to obtain salt, a valuable resource at that time. For this purpose, the brine was concentrated by what is known as an "igneous method", that consisted on evaporating the waters by heating on the fire and finally obtaining salt cakes by the repetitive addition of more brine (Abarquero Moras et al., 2017).

During the 1970´s decade Villafáfila lakes were threatened by the wetland desiccation policy of the Spanish Government for agricultural purposes. Some trenches were excavated for desiccating Laguna Salinas, that disappeared almost completely (González-Bernáldez, 1992). Nowadays, Villafáfila lakes area is a natural reserve, an area of special protection for birds (ZEPA), a Site of Community Importance (SCI) for the European Union, and it is included in the intergovernmental RAMSAR treaty for conservation of wetlands. Villafáfila lakes is an ecosystem developed on a steppe landscape with saline grasslands, that constitutes the habitat of one of the world largest population of Great Bustard (*Otis tarda*), and is the place for wintering of a large number of ducks and geese. The salinity of the lake waters is one of the key issues for the existence of this ecosystem and understanding its interaction with groundwaters is essential to maintain the equilibrium with human water consumption activities such as agriculture and livestock. This research, focused on the hydrogeology of the lakes basin, can help characterize the present situation of the area, analyze the lake - groundwater interaction and take informed decisions for managing the environmental protections.

2. Hydrogeological background

2.1. Duero basin

Villafafila lakes are located in the Duero river hydrological basin that occupies the Northern Spanish Meseta which has an altitude of 700 to 800 m above sea level (masl) along the central axis of the Duero River. This low relief area is dominated by Cenozoic continental sedimentary rocks surrounded by mountain ranges, about 2400 masl, constituted mainly by pre-cenozoic rocks. The northern hydrological basin divide locates in the Cantabrian Mountains, constituted mainly by Precambrian and Paleozoic metamorphic and sedimentary rocks, and a Mesozoic sedimentary cover, consisting of evaporites, limestones and clastics, that forms a discontinuous marginal fringe around the Cenozoic infill of the Duero basin (Fig. 1). To the East, it is bounded by the Iberian Ranges, with a similar rock record but with a thicker Mesozoic succession. The Spanish Central System represents the southern divide, mainly consisting of Paleozoic plutonic and metamorphic rocks with an Upper Cretaceous sedimentary cover at the contact with the Cenozoic succession. The western margin (Iberian Massif) is dominated by Precambrian and Paleozoic metamorphic and plutonic rocks, surrounded by a discontinuous fringe of siliceous sandstones attributed to the Upper Cretaceous (Corrochano and Armenteros, 1989; Corrochano et al., 2006).

The Cenozoic succession forms low relief areas and is constituted by continental detrital sedimentary rocks in the periphery and by non-marine carbonates (mainly limestones) and evaporites (mainly gypsum) towards the center (Alonso-Gavilán et al., 2004; Armenteros et al., 2002). This rock succession is the main aquifer system in the region. The hydrological basin is drained by the Duero river and its tributaries towards the west (Fig. 1). Close to Zamora city, the Duero river abandons the Cenozoic succession and dissects the plutonic and metamorphic rocks of the Iberian Massif till its outlet in the Atlantic Ocean.

The Cenozoic aquifer system of the Duero basin is one of the largest in the Iberian Peninsula (Navarro Alvargonzález et al., 1993). It has an extension of about 45,000 km^2 and its thickness is about 1000–2000 m, reaching 3500 m in some parts, like in the Almazán basin and in the northern basin margin (Herrero et al., 2004; Huerta et al., 2011).

Regional groundwater flow pattern in the Duero aquifer system (Fig. 1) comes from the basin margins, showing an increase in electric conductivities and Cl^- content downflow, towards the Duero river where brackish groundwaters discharge (IGME, 1980).

The aquifer recharges mainly by rain infiltration and by subterraneous flows coming from the mountain ranges. In the Esla-Valderaduey area (north of the Duero River), where Villafáfila's lakes occur, recharge areas are mainly the interfluves, and local groundwater flows towards the rivers Cea, Esla and Valderaduey, tributaries of the Duero river from the north (IGME, 1980). In the Villafáfila groundwater mass, deep boreholes (> 150 m) are flowing artesian wells with specific discharges about 1 L/s like in Villalpando (Navarro Alvargonzález et al., 1993).

2.2. Villafáfila area

Villafáfila's lakes are located in a low slope reach at 677 masl, at the bottom of a wide valley surrounded by hills that reach up to 730 masl, at

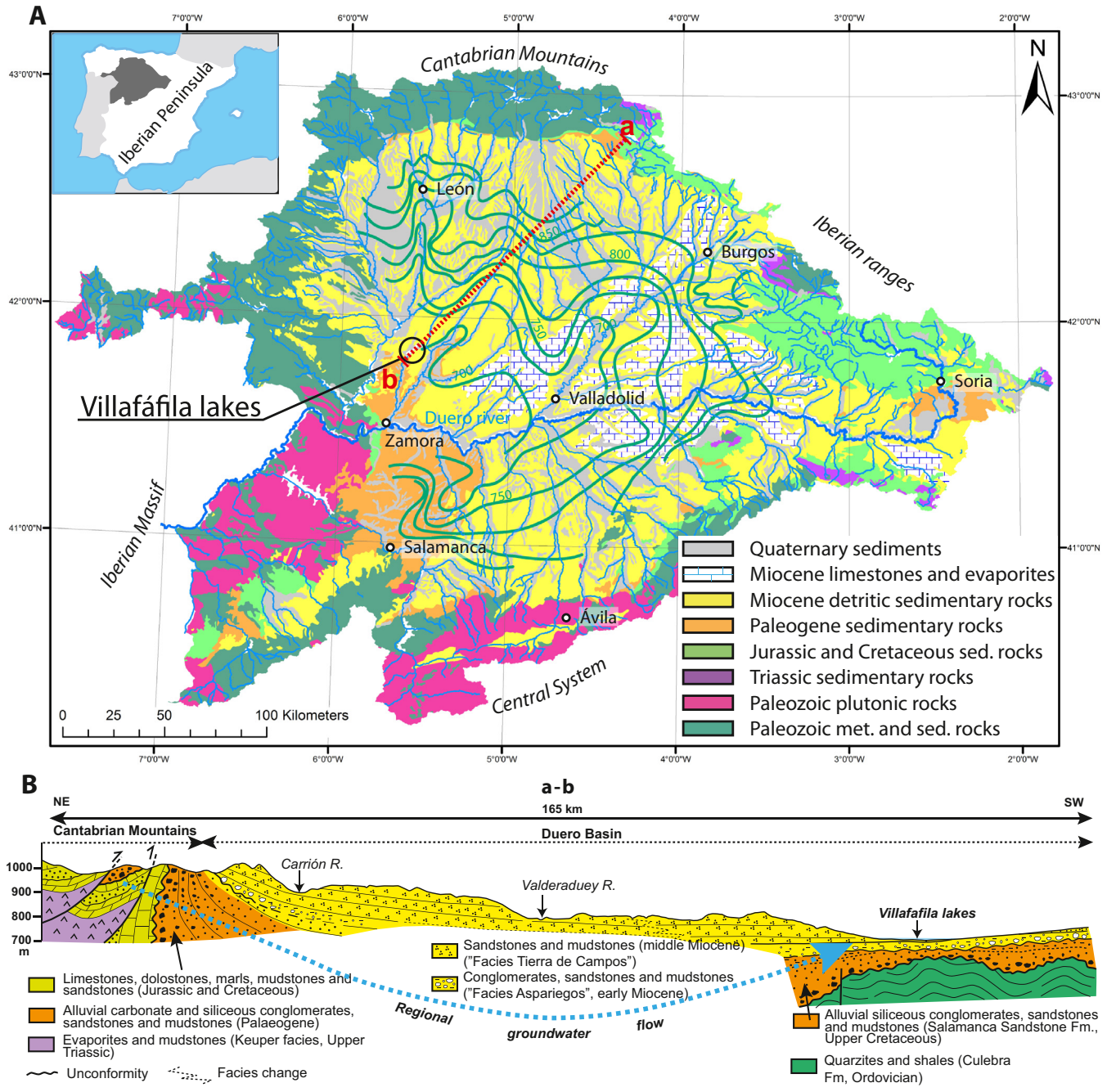

Fig. 1. A) Geological setting of the Duero river hydrological basin and location of Villafáfila's lakes. Green lines are the water table map of the Cenozoic Duero aquifer system obtained from boreholes screened at depths greater than 200 m (reference piezometry, >200 m) (CHD, 2009). B) Cross section of the Duero basin from the Cantabrian Mountains to Villafáfila lakes area. See location in (panel A).

the head of the Salado river, tributary of the Valderaduey. The slope of the Salado river increases downstream from the locality of Villarrín de Campos towards the south. The hydrological basin of the lakes has an area of 156 km^2 till Villarrín de Campos, with several main lakes aligned northeast to southwest: Barillos (118 ha), Salina Grande (194 ha) and San Pedro (70 ha) lakes (Fig. 2). Salinas lake was drastically disrupted after it was dredged in 1972. These ephemeral lakes are normally flooded from November to June and dry out from June to October (Fig. 3). There are no salt crusts on the lake bottoms, but there are efflorescences in the lake sediments and in the lowland areas surrounding the lakes during the summer. The streams that flow into the lakes are normally dry, only carrying water during strong storms events. Drainage is normally through the shallow groundwaters occurring in the lowlands that surround the lakes (Fernández Pérez and Cabrera Lagunilla, 1987). Several springs close to the lakes supply low water discharges (about 0.2 L/s each). Overall, the Villafáfila hydrological basin drains into the Salado river at Villarrín de Campos, and despite the Salinas lake having been artificially drained, the surficial discharge is very low. Instead, the main outflows correspond to groundwater discharge (Fernández Pérez and Cabrera Lagunilla, 1987). Lake bottoms accumulated Holocene sediments that reach up to 9 m thick, as observed during the construction of a piezometer in Salina Grande, and consist on clays, silts and sands with carbonate nodules (López Sáez et al., 2017; Santisteban et al., 2003). These Holocene sediments behave as an aquitard with hydraulic conductivity of 0.05–0.1 m/d. This aquitard lies directly on top of Miocene heterogeneous beds of siltstones,

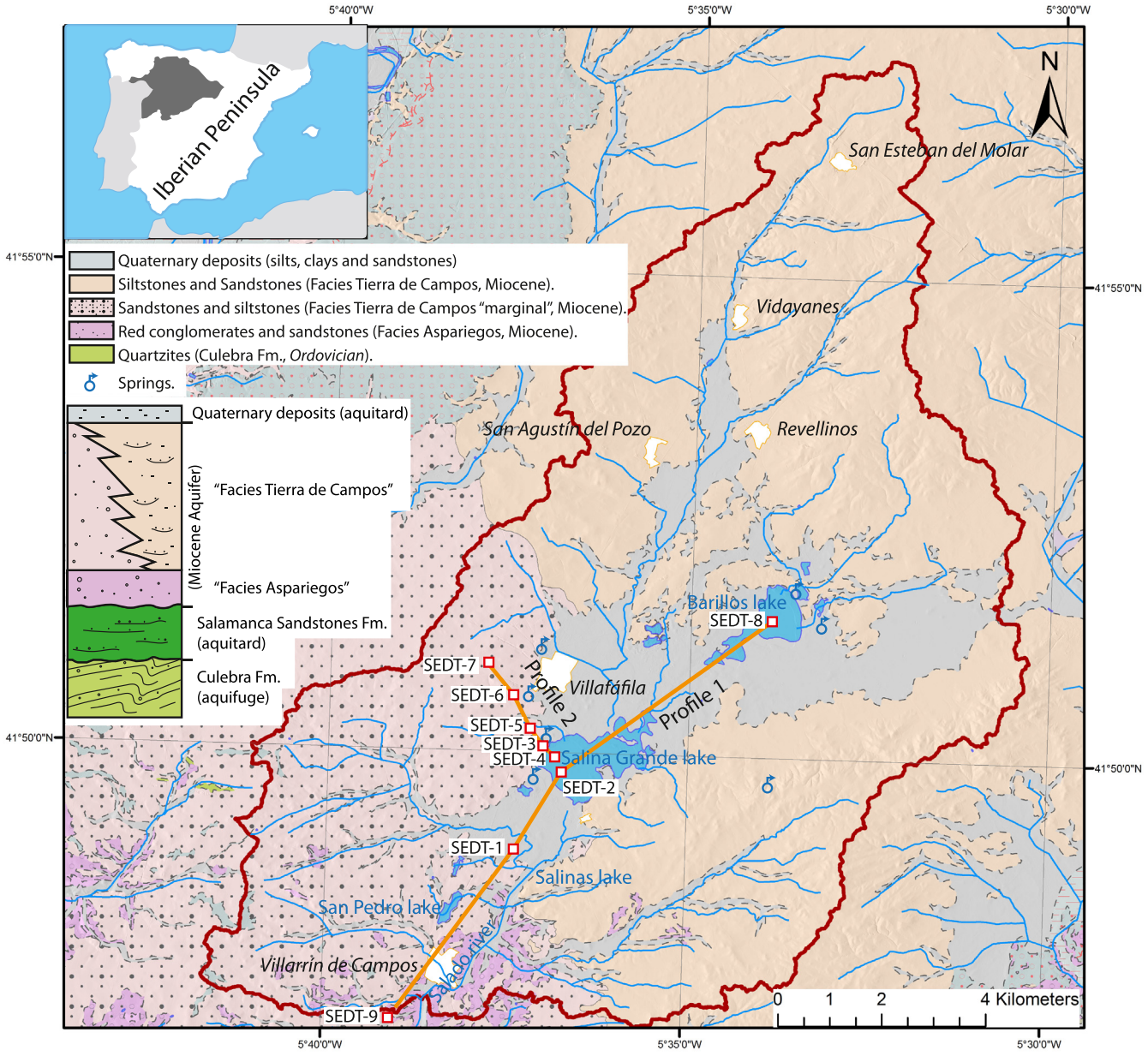

Fig. 2. Geological setting of the río Salado and the Villafáfila lakes hydrological basin. Orange lines mark the location of the TDEM profiles and the squares points to location of the TDEM stations.

sandstones and conglomerates which crop out on the surrounding hills, conforming the "Facies Tierra de Campos" Unit, that towards the west show proximal coarser terrigenous deposits (Martín Serrano and Barba Martín, 1979; Martín Serrano and Piles Mateo, 1982) (Fig. 2). On the southern edge of the lacustrine area crops out the basal Miocene unit ("Facies Aspariegos"), stratigraphically below "Facies Tierra de Campos", formed by conglomerates, sandstones and siltstones (Fig. 2). The thickness of the Miocene aquifer is variable because it adapts to a palaeorelief, but normally exceeds 100 m in the Villafáfila area (IGME, 1980). Its permeability is medium to high (0.1–100 m/d) (IGME-DGA, 2009). The Salamanca Sandstone Formation (Upper Cretaceous) underlies the Miocene units and crops out discontinuously along the western margin of the Duero basin, and can be seen at surface, underlying the Miocene Units, 8 km west of Villafáfila's lakes. It consists of iron-mottled opal-cemented sandstones and conglomerates with intercalated silcretes (Alonso-Gavilán et al., 2004; Blanco et al., 2008) and it has low permeabilities. The older rocks in the area are the Ordovician quartzites and shales (Culebra Fm) of the Iberian Massif that crop out to the west of Villafáfila, forming northwest-southeast trending folds in the Sierra de la Culebra. The permeability of these rocks is very low, but they show rock fracturation.

2.3. Climate in Villafáfila

Average annual precipitation in Villafáfila for the period 2015–2019 is 330 mm, mostly scattered from October to May. The summer (June to October) is dry and average monthly precipitation does not exceed 30 mm, being less than 14 mm in July and August (Fig. 3). Mean annual temperature in the area is 13 °C with the lowest values in January (4.3 °C) and the highest in July (22.7 °C) (AEMET, 2020). Mean annual lake evaporation, measured from evaporation tanks, is 720 mm. Mean annual real evapotranspiration (ETR) for the period 2015–2019 is 237 mm. Annual ETR has been obtained from the sum of the monthly ETR. Monthly ETR, soil deficit and surplus have been calculated using the exponential method for soil water balance (Thornthwaite and Mather, 1955) for the period 2015–2019 assuming a field capacity of

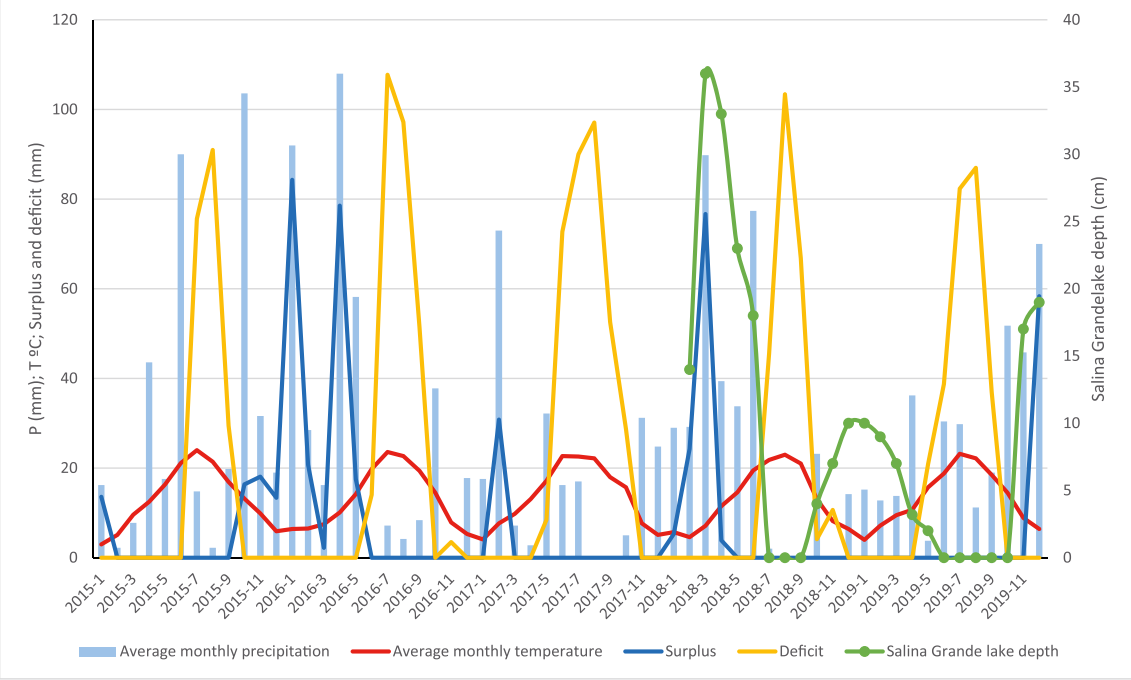

Fig. 3. Five years time series of average monthly precipitation and temperature obtained from Villafáfila's meteorological station. Surplus and deficit have been obtained using the exponential Thornthwaite and Mather (1955) method, for a field capacity of 60 mm. Salina Grande lake level record spans only from February 2018 to December 2019.

60 mm (Table SM 1 - Suppl. Mat.). From October to April, precipitation exceeds evapotranspiration, favoring the soil surplus, the aquifer recharge and the rise of the lake level (Fig. 3). During summer, evapotranspiration exceeds precipitation, resulting in soil water deficit that coincides with the decrease of lake level and its final drying out (Fig. 3).

3. Methodology

Surface and groundwaters were sampled from lakes, springs, boreholes (depths >40 m) and dug wells (depths <40 m) (by sampler or by pumping) in the Villafáfila hydrological basin. Most of the boreholes and dug wells are screened in the Miocene aquifer. Depth to water table, pH, electrical conductivity (EC), temperature and alkalinity were measured in the field. pH was measured with a Hanna HI 9023 pH-meter calibrated with pH buffers. EC and temperature were measured with a Hanna HI 9835 m and probe. Alkalinity was determined using drop titration and appropriate reagents. Samples were collected in screw-cap HDPE bottles filled to overflowing and stored refrigerated at 4 °C until analysis. Major and minor cations (Al, Ca, K, Mg, Na, Si; ppm) were analyzed on field-acidified water samples (16 N HNO_3 to pH ≈ 2) using ICP-OES (Ultima II from Jobin Yvon) and minor and trace elements (Li, Sr; ppm) by use of an ICP-MS (Elan 6000 from Perkin-Elmer) at the Servicio General de Análisis Químico Aplicado, Universidad de Salamanca, Spain. SO_4^{2-} NO_3^- and Cl^- concentrations were determined with a Hatch DR2800 spectrophotometer after addition of appropriate reagents and titration.

Additionally, monthly precipitation was collected according to the method of IAEA-WMOs GNIP Network (www.naweb.iaea.org/ih/IHS_resources_gnip_faq.html, accessed on 2020/10/07), employing a home-made pluviometer emplaced within the grounds of the official "Villafáfila" meteorological station, operated by the Spanish Meteorological Agency (AEMET) and located within the premises of Villafáfila's Natural Reserve "park house". Evaporation was prevented by adding to the pluviometer a thin (~2 mm) layer of paraffin oil. The sampling period extended for 24 months, from October '2016 to September '2018, both included, although the number of results reported is fewer than 24, since there was no precipitation in some of the summer months.

Stable Oxygen isotope analyses on water ($\delta^{18}O_{water}$) were done by equilibration with CO_2, using a Multiflow (Micromass) equilibrium device. D/H ratios were determined on H_2 gas obtained by the Cr-reduction method, using a EuroVector EA3000 elemental analyzer. Isotopic ratios were measured on a continuous flow Isoprime (Micromass) mass spectrometer coupled on line to the preparation devices. Water samples for $\delta^{34}S_{SO4=}$, $\delta^{18}O_{SO4=}$ analyses were filtered through 0.45 μm nylon filters. Water-soluble sulphate was precipitated by addition of 10% $BaCl_2$ solution to the previously acidified (to pH ≈ 2) water, essentially following the original method of Rafter (1967), as amended by Sakai and Krouse (1971) and Mizutani and Oana (1973). The $BaSO_4$ precipitate was separated from the solution by filtering through Whatman #42 filter (125 mm diameter), washed with distilled water, and air-dried. Sulphur isotope analyses ($\delta^{34}S$) were done on SO_2 produced off-line following the method of Robinson and Kusakabe (1975), with modifications for sulphates by Coleman and Moore (1978). Isotopic ratios were determined on a dedicated dual inlet SIRA-II (VG-Isotech) mass spectrometer. The oxygen isotopic composition of the $BaSO_4$ ($\delta^{18}O_{SO4=}$) was measured on CO obtained by pyrolysis on a EuroVector EA3000 elemental analyzer, coupled on-line to an Isoprime continuous flow mass spectrometer. Isotopic ratios are reported in the usual "δ" notation as per mil (‰) deviations from V-SMOW ($\delta^{18}O_{H2O}$, δD_{H2O}, $\delta^{18}O_{SO4=}$), CDT ($\delta^{34}S_{SO4=}$). Radiocarbon dating was performed by Beta Analytics Inc. on a single sample DIC of groundwater and is reported both as percent modern carbon (pMC) and fraction of modern (F14C). Dissolved inorganic carbon (DIC) extraction consisted of injecting sample water into an acid bath attached to an evacuated collection line. pH was reduced to <1 and evolved CO_2 was dried with methanol slush and collected in liquid nitrogen. CO_2 was then graphitized over cobalt in a hydrogen atmosphere to produce the target for AMS. Reported radiocarbon results are relative to NIST SRM—4990C.

Time-domain electromagnetic (TDEM) surveys allow measuring the resistivity (ρ) distribution at depth. Resistivitiy depends on factors such as porosity, rock resistivity, water resistivity (inverse of electric conductivity) and water saturation (Merritt et al., 2016; Waxman and Smits, 1968). Nine sites of TDEM surveys were carried out with a TerraTEM

(MONEX GeoScope Ltd.) transient electromagnetic survey system on the summer of 2019, with the geophysics company Técnicas Geofísicas S.L. Four sites were performed with 150 × 150 m side square single loops to construct the NE-SW profile parallel to the lakes orientation. The other five sites were done with 50 × 50 m side square single loops situated in a line perpendicular to the valley axis.

4. Results

4.1. Groundwater head

The regional water table map in the Esla-Valderaduey interfluves in the northwestern sector of the Duero basin aquifer system indicates that regional groundwaters (depths >200 m) come from the northeast and flow towards the Duero river in the Zamora city area (Fig. 1). Hydraulic Gradient in the upflow areas, from the Cantabrian Mountains to Villafáfila is 0.003 and from Villafáfila to Zamora reduces to 0.0015 (Fig. 1). The local water table map in Villafáfila hydrological basin, obtained from dug wells (depths <40 m) and springs, was measured in September 2017. It shows a northeast-southwest groundwater flow component and a lateral component from the hills that surround Villafáfila towards the lakes (Fig. 4A). The lowlands where the lakes occur show very gentle gradients (0.001) and a shallow (decimetric depths) groundwater table, while in the hills the gradient is 0.01 and the groundwater table is about 7 m deep. In the upper part of the hills wells (screened at depths >40 m) show lower hydraulic heads than dug wells (screened at depths <10 m) (Fig. 4B). Both opened in the Miocene aquifer. At the toe of the hills and at the margins of Salina Grande and Barillos springs and flowing artesian wells (depths >40 m) occur (Fig. 4A). The flowing artesian observation well (SGR- 3) screened from 10 to 1 m depth, drilled in the bed of Salina Grande (Fig. 4A, C), evidenced that hydraulic head at 10 m depth was 677.6 masl (0.4 m above lake bottom) during September 2020. On the other hand the observation well SGR-2, also within Salina Grande (200 m apart from SGR-3) (Fig. 4C), screened at 3.5 m depth had a hydraulic head of 676.6 masl., (0.6 m below lake bottom) during September 2020. Calculated vertical gradients

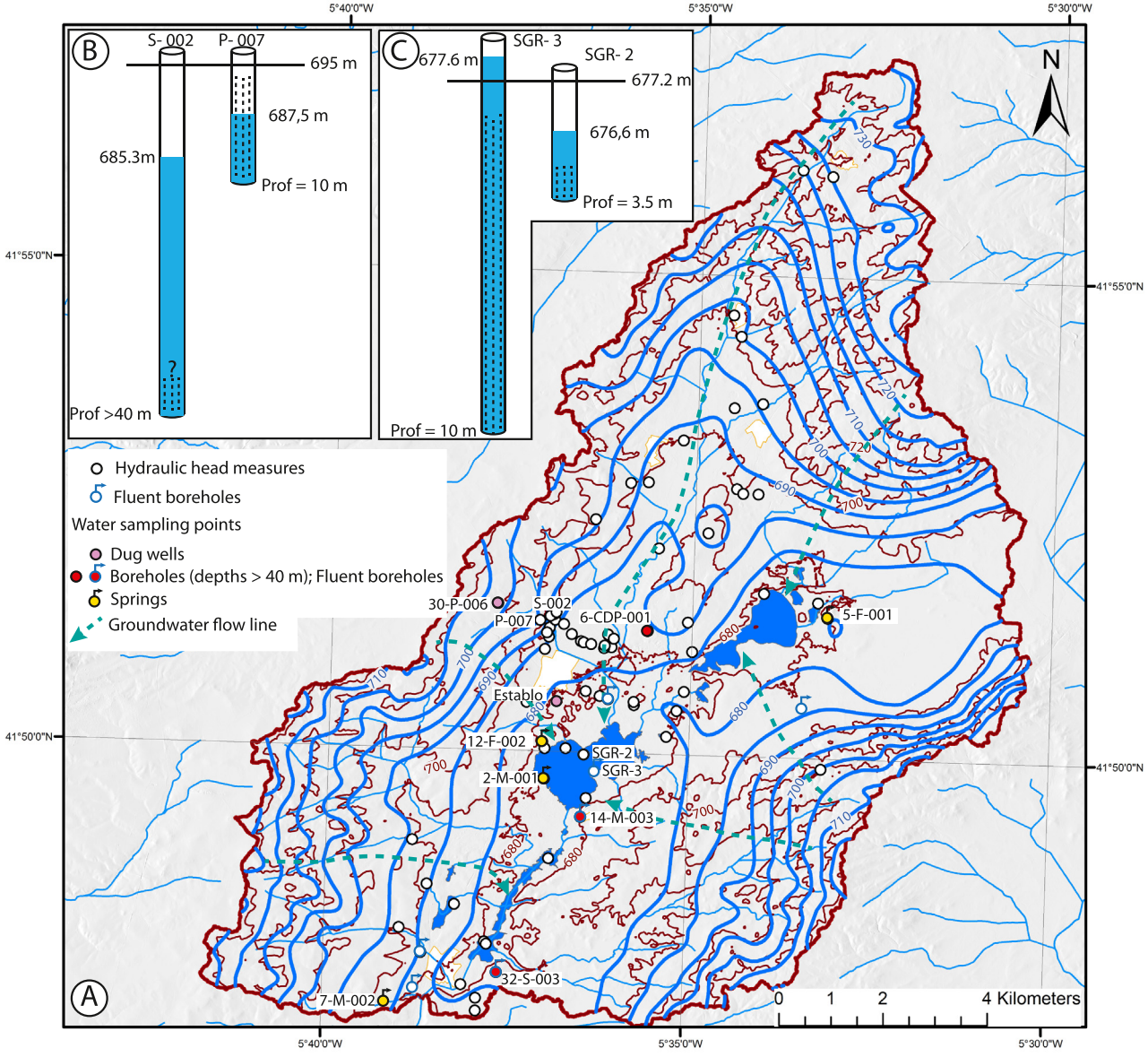

Fig. 4. Water table map (blue lines) of the Villafáfila lakes hydrological basin. Brown numbered lines are the terrain elevation. A) Water table map obtained from dug wells (depths <40 m) and springs, in September 2017. B) Hydraulic head differences in wells screened at different depths located on the hills. C) Hydraulic head differences in wells screened at different depths located on the bed of Salina Grande lake, September 2020. (For interpretation of the references to color in this figure legend, the reader is referred to the online version of this chapter.)

of hydraulic heads should be corrected using the environmental hydraulic head (Lusczynski, 1961), but the salinities of Villafáfila groundwaters (see Section 4.2.1) make this correction negligible with respect to the hydraulic head differences. During the dry season (September 2020), when the lakes were completely dry, the vertical gradient is 0.14. During winter and spring, when the lake level is high, the vertical gradient decreases notably but SGR-2 cannot be measured. Outside the main lakes, between Barillos and Salina Grande, permanent small ponds occur. These ponds, dominated by palustrine vegetation, remain flooded during the dry season, while the main lakes are dry. The water level in these ponds is higher (0.2–1.5 m) than the groundwater table in Salina Grande lake and sometimes overflows to this latter.

4.2. Water chemistry

4.2.1. General patterns

Shallow and deep groundwaters show contrasting values for major physicochemical parameters, both as it regards absolute values and their variation along the year (Table SM 2 - Suppl. Mat.): deep groundwaters have relatively constant temperatures between $T = 15$–18 °C all year round, pH ≈ 7.2 and there are no major salinity variations (TDS = 3200–5000 mg/L; EC = 4600–6400 μS/cm). Shallow groundwaters around Villafáfila, however, have contrasting T, pH, TDS and EC, that are different in the hills (pH = 7.5, TDS = 256 mg/L, EC = 400 μS/cm) and in the plains surrounding the lakes (pH = 8.6, TDS = 1300–3850 mg/L, EC = 2000–6000 μS/cm), with $T = 10$–18 °C. Variation is even more marked in lake water itself, with pH = 7.8–10.0, $T = 7.5$–23 °C, TDS = 800–6200 mg/L and EC = 1000–10,000 μS/cm, increasing as the lakes evaporate or at the beginning of the winter. During summer drying, shallow groundwater underneath lake beds (i.e., at piezometer SGR-2, Fig. 4) shows highest values of TDS (12–27 g/L) and EC (19000–42,000 μS/cm).

4.2.2. Major components

Major components in lake and groundwaters (Table SM 2 - Suppl. Mat.) allow identifying 3 different water types (Fig. 5): Type 1) low salinity groundwaters dominated by Ca^{2+} (up to 50% of total cations) and HCO_3^-; Type 2) mixed groundwaters dominated by HCO_3^-, Cl^- (about 50%) and Na^+ (>70% of cations); Type 3) high salinity waters dominated by Na^+ and Cl^- (>70% of both ions) (Fig. 5). Type 1 corresponds with the groundwaters sampled in dug wells located in the hills surrounding the lakes. Type 2 generally occurs at the toe of the hills in dug wells and springs. Type 3 has been identified in lake waters, springs close to the lake margins and boreholes deeper than 40 m. Boreholes and observation wells close to or within the lakes show type 3 waters at depths shallower than 40 m.

Ionic relationships (expressed in meq/L) are a guide to the behavior of lake and groundwaters in the Villafáfila basin (Fig. 6 A-F): Na^+ and Cl^- show good correlation ($R^2 = 0.96$), (Fig. 6 A) with Na^+/Cl^- ratios close to 1 (0.98) (Fig. 6 A, E). Dug wells in the surrounding reliefs, and the springs at their toe show lower concentrations of Na^+ and Cl^- than the deep groundwaters (boreholes >40 m and the springs surrounding the lakes). The spring 5-F-001 show higher Na/Cl ratios than other samples (Fig. 6E). Na^+ and Cl^- concentrations in lake waters are variable. During winter to spring periods, when water levels are high, Na^+ and Cl^- concentrations are lower than those of deep groundwaters. In contrast, when the lakes are concentrated by evaporation (end of spring) or at the beginning of the winter, when starts to be filled up, some lake waters show higher Na^+ and Cl^- values than deep groundwaters.

Ca^{2+} and Cl^- show a poorer correlation ($R^2 = 0.72$) than Na^+ and Cl^- (Fig. 6B). Most of the samples (except for dug wells located in the hills) have Ca^{2+}/Cl^- ratios lower than 1 (0.099) (Fig. 6 F). Ca^{2+} and SO_4^{2-} have poor correlation ($R^2 = 0.66$) and Ca^{2+}/SO_4^{2-} ratio is 0.46, and is even lower for the more evaporated lake waters, which are depleted in Ca^{2+} (Fig. 6 C). The Mg^{2+}/Ca^{2+} ratio is mostly <1 (about 0.5 for the whole samples), except for some lake waters that show Mg^{2+}/Ca^{2+} ratios that slightly exceed 1 (Fig. 6 D).

Saturation indices for several minerals have been calculated with PHREEQC (Parkhurst and Appelo, 2013) (Table SM 3 - Suppl. Mat.). Lake waters, especially those that have suffered evaporation, are oversaturated with respect to dolomite, calcite and aragonite, but are highly undersaturated with respect to gypsum and halite. Most of the deep and shallow groundwaters (springs, boreholes and dug wells) are undersaturated in all those minerals.

4.2.3. Stable isotopes

Isotopic ratios obtained are reported in Table SM 2 - Suppl. Mat. and Fig. 7A and B.

Precipitation samples collected span two consecutive meteorological years (October '2016 to September '2017 and October '2017 to September '2018), that provided 21 values, ranging from $\delta^{18}O = -11.7‰$ in November '2016 to $\delta^{18}O = -3.3‰$ in July '2017, and from $\delta D = -84.8‰$ (November '2016) to $\delta D = -18.9‰$ (in May '2017; the next heaviest value, at $\delta D = -23.6‰$ was also measured in the sample corresponding to July '2017). There was no rain in September '2017 and August '2018, and the sample corresponding to July '2017 (29.2 L/m^2) was lost.

When plotted on a $\delta^{18}O$ vs δD graph (Fig. 7A) precipitation samples analyzed plot very close to the Global Meteoric Water Line (GMWL, as defined by Craig, 1961), although slightly below it (as it corresponds to a semiarid area; accumulated precipitation for the 2016–17 meteorological year was 235.6 mm, and 396 mm for 2017–18; data from AEMET) and can be used to define the local Villafáfila meteoric water line (LMWL) as $\delta D = 7.3\ \delta^{18}O + 2.1$.

As far as possible, lake water was sampled seasonally. However, the natural dynamics of these very shallow lakes result in them drying out for extended periods, and as such, surface water was not always available for sampling. Measured values range from $\delta^{18}O = -9.3‰$, $\delta D = -67.9‰$ (Laguna Salina Grande, December '2017) to $\delta^{18}O = +4.8‰$, $\delta D = +5.9‰$ (Laguna San Pedro, June '2016). When plotted on the ^{18}O vs δD graph (Fig. 7A) oxygen and hydrogen isotopic values strongly correlate ($\delta D = 5.2\ \delta^{18}O - 14.1$; $R^2 = 0.97$, for $n = 21$), defining an evaporation line with lower slope than LMWL, and a negative value of deuterium excess.

Deep groundwaters, sampled from deep boreholes (some of which are flowing artesian wells) and springs located in the lake margins have remarkable constant (both in space and time) $\delta^{18}O$ and δD values, averaging $\delta^{18}O = -9.8 \pm 0.3‰$ and $\delta D = -69.8 \pm 2.8‰$, for $n = 26$. On the $\delta^{18}O$ vs δD graph of Fig. 7A these waters plot around the intersection between GMWL and LMWL, at values that are lower than the intersection of the evaporation line defined by lake waters with either GMWL or LMWL. Deep groundwaters have sulphates whose $\delta^{18}O$ varies from +10.8 to +17.8‰, and $\delta^{34}S$ from +13.4 to +18.6‰. It is worth noting, within this set of samples, that the lowest $\delta^{18}O$ and $\delta^{34}S$ values obtained all correspond to the same station, sampled over time. This station (6-CDP-001, in Table SM 2 - Suppl. Mat. and Fig. 4) is a deep borehole heavily pumped all year round to maintain water in an artificial pond within the premises of the Natural Reserve's Park House, and as such it differs from any other boreholes sampled, none of which are regularly pumped. If 6-CDP-001 borehole is not considered, the range of values reduces considerably, to $\delta^{18}O = 12.8$ to 17.8‰ and $\delta^{34}S = 16.8$ to 18.6‰.

The three samples of shallow groundwaters (dug wells) vary between $\delta^{18}O = -9.4$ to −6.3‰ and $\delta D = -68.3$ to −50.3‰. When plotted on Fig. 7A, a linear trend with a lower slope than LMWL is observed ($\delta D = 6.4\ \delta^{18}O - 8.3$), hinting that these samples were also subjected to evaporation. Thus, if these samples were included in a single regression along the lake waters, the new defined evaporation line ($\delta D = 5.3\ \delta^{18}O - 14.1$) would be indistinguishable from that defined by the lake water alone ($\delta D = 5.2\ \delta^{18}O - 14.1$).

Sulphate isotopes from surface (lake) waters (Fig. 7B) gave $\delta^{18}O_{SMOW}$ values that ranged between $\delta^{18}O = +10.3$ to +20.1‰, although we have

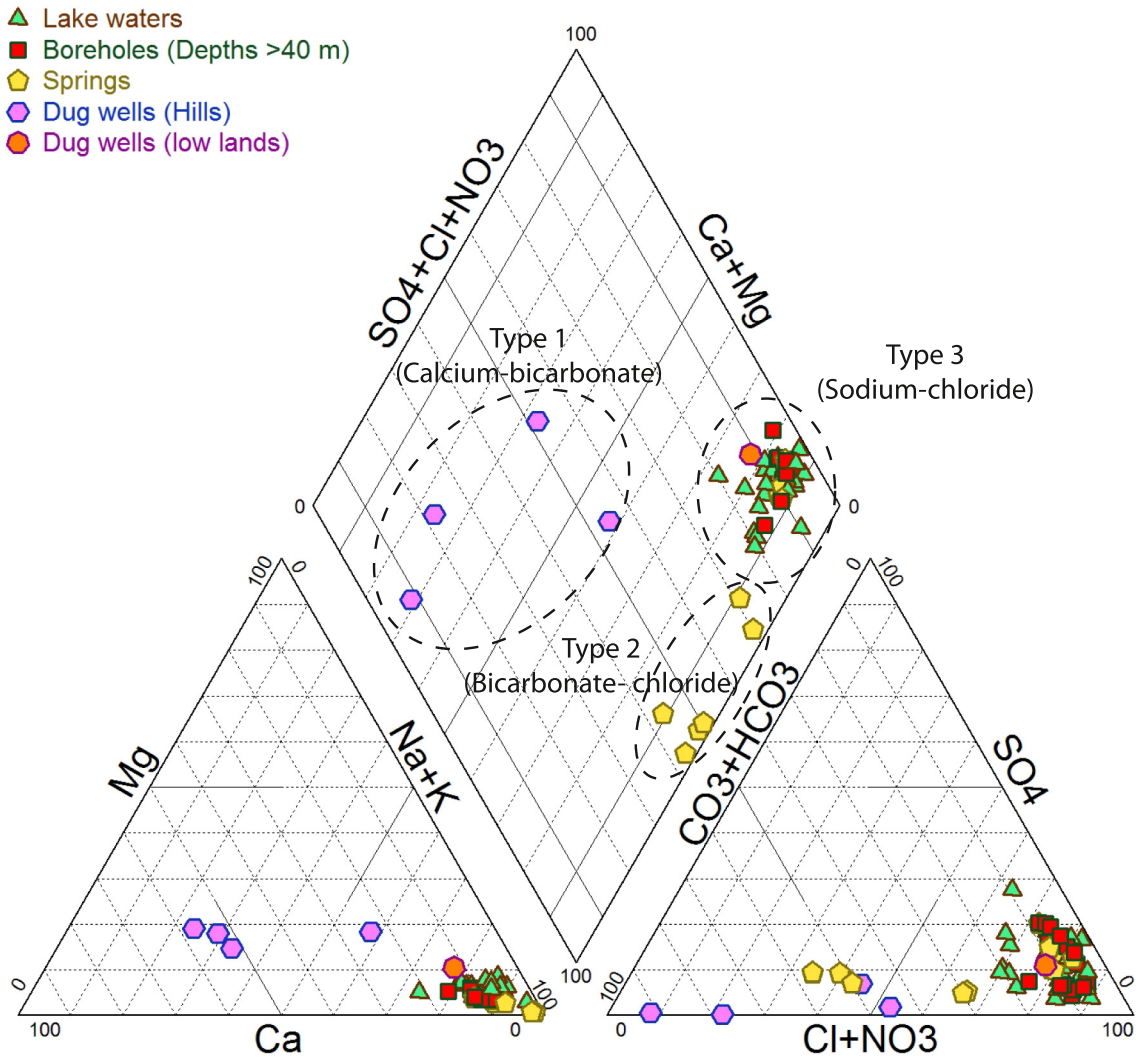

Fig. 5. Piper diagram showing the chemical composition of lake and groundwater in Villafáfila watershed. Three types of waters have been identified according to their composition. Data are shown in Table SM 2 - Suppl. Mat.

reasons to consider this higher value as an outlier. Disregarding that sample the range reduces to $\delta^{18}O = +10.3$ to $+16.2‰$. The range for $\delta^{34}S_{CDT}$ spans from $+8.4$ to $+25.8‰$. The upper end of this range results from three samples with $\delta^{34}S$ around $+25‰$, sampled on 16/06/2016. Without these samples the $\delta^{34}S$ values range from $+8.4$ to $+18.8‰$. The lower end of the range was measured on station 11-AS-001, during the winter (31/01/17) and one of the highest $\delta^{34}S$ values was taken at the same station but 7 months later (16/06/16).

4.2.4. Mean residence time of deep groundwaters,

Single-sample radiocarbon dating of deep groundwater was obtained from 32-S-003 borehole at 60 m depth, close to the locality of Villarrín (Fig. 2). DIC measured activity was 1.24 +/− 0.04 pMC (Table 1). Radiocarbon ages can show wide ranges depending on the estimation of $^{14}C_0$, but single-sample models like Pearson's (Ingerson and Pearson, 1964; Pearson and White, 1967) and IAEA's (Gonfiantini, 1972; Salem et al., 1980) are considered to include all common processes and can be used in wide ranges of ^{13}C values (Han and Plummer, 2016). According to Pearson's model initial activity $^{14}C_0$ is 18.57 pMC, while according to IAEA's model $^{14}C_0$ is 32.31 pMC. The ages calculated using the measured DIC activity and the Pearson and IAEA initial activities are 22.3 Ka. and 28.9 Ka BP respectively, but the use of other models could provide older ages.

4.3. Geophysics

Time domain electromagnetic (TDEM) profiles measure resistivity changes of rocks and pore waters below the surface. Profile 1 is oriented NE-SW, parallel to the lakes alignment (Fig. 2) and reaches 300 m below the terrain surface. Profile 2 is perpendicular to profile 1 and goes from the hills close to Villafáfila village to Salina Grande lake (Fig. 2), reaching about 200 m below the surface. Profile 1 evidences the occurrence of several geoelectric units (GE) with different geometries and resistivities (Fig. 8A). From base to top, GE-1 has the highest resistivities (70 Ohm/m) and its upper part appears 120 m below the surface (580 masl) in the SEDT 1 station (Between San Pedro and Salina Grande lakes). GE-1 slopes gently dipping to the NE in its NE side while its SW side is more abrupt. On SEDT 8 station, below Barillos lake, the top of GE-1 is deeper than 300 m (below 400 masl). GE-2, with resistivities about 30 Ohm/m, lies above GE-1. It has tabular geometry and its thickness is about 70 m. This unit dips gently northwards, from SEDT-2 to SEDT-8 (below Salina Grande and Barillos lakes), and is partially truncated from SEDT2 (Salina Grande) towards the SW. GE-3 lies on top of GE-2 in profile 1 and has low resistivities ranging between 3 and 10 Ohm/m. In profile 2 GE-3 appears at the lower part of the profile and its recorded thickness is variable, reaching up to 150 m (Fig. 8B). GE-4 shows variable resistivities between 10 and 20 Ohm/m in profile 1

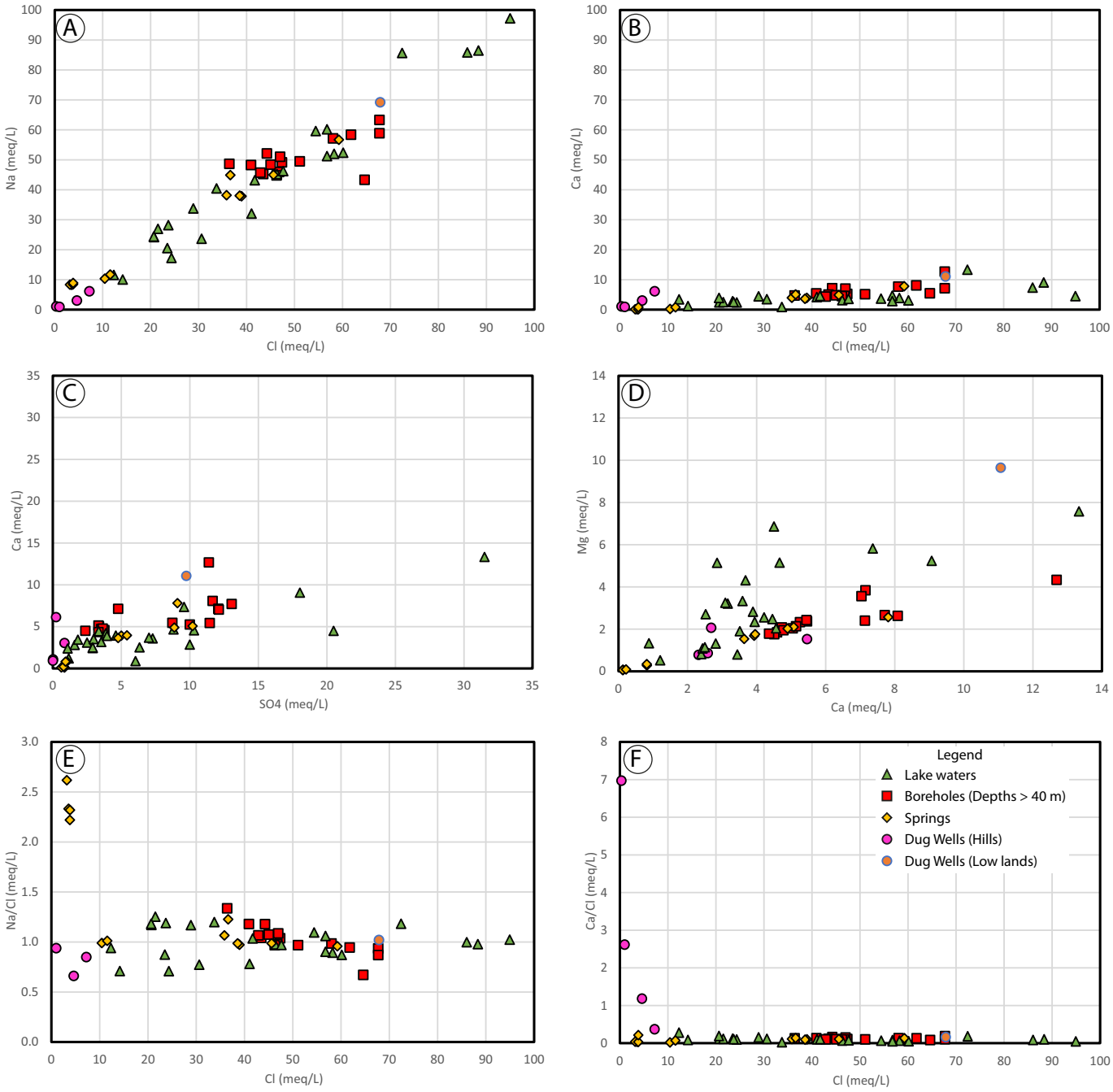

Fig. 6. Relationships between A) [Na^+] and [Cl^-]; B) [Ca^{2+}] and [Cl^-]; C) [Ca^{2+}] and [SO_4^{2-}]; D) [Mg^{2+}] and [Ca^{2+}]; E) [Na^+]/[Cl^-] and [Cl^-]; F) [Ca^+]/[Cl^-] and [Cl^-]. Data are shown in Table SM 2 - Suppl. Mat.

(Fig. 8A), and is sandwiched between low resistivity (<10 Ohm/m) units GE-3 and -5. In profile 2, below the hills (stations SEDT 6 and 7), GE-4 corresponds with the transitions between the low resistivities of GE- 3 and the high resistivities of GE-6 (Fig. 8B). GE-5 has low resistivities (2–10 Ohm/m) and appears just below the terrain surface, with tabular geometry. Below SEDT-2 (Salina Grande lake) and SEDT-8 stations (Barillos lake) its thickness is about 20–30 m. Towards the southeast of SEDT-2 (Salina Grande lake) GE-5 sinks below 30 m depth and increases progressively its resistivity values towards the SW (Fig. 8A). GE-6 is a high resistivity unit located under the hills surrounding the lakes. Measured resistivity is about 30 Ohm/m; its thickness below the hill's surface is about 30 m and decreases towards the toe of the hills (Fig. 8B).

5. Discussion

5.1. TDEM profiles interpretation

This research uses the TDEM technique to study groundwaters in lake basins because of its sensitivity to low resistivity changes (Pedrera et al., 2016; Tchouta et al., 2019). This method is useful to pinpoint salinity changes not only in aquifers related to saline lakes, but in coastal aquifers as well (Al-Garni and El-Kaliouby, 2011; El-Kaliouby, 2020). It has also been used to determine aquifer geometries (Ruiz-Constán et al., 2015). GE units defined correspond with the different units of the rock record and with the different salinity content of their groundwaters. The lowermost unit GE-1, which has high resistivity

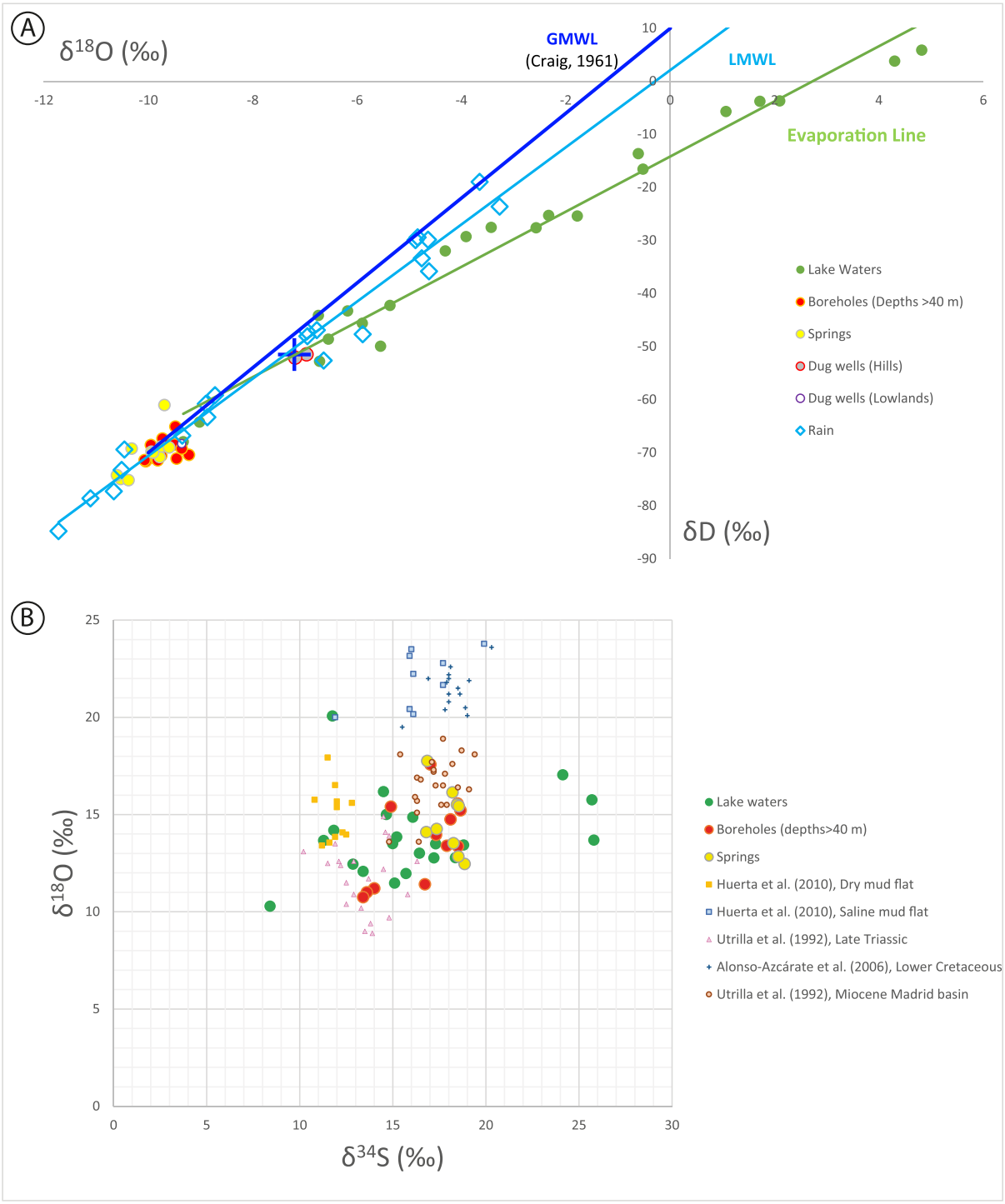

Fig. 7. Stable isotopic composition A) δD_{SMOW} Vs $\delta^{18}O_{SMOW}$ of rainfall, lake waters and groundwater in Villafáfila area. GMWL is the Global Meteoric Water line (Craig, 1961). LMWL is the Local Meteoric Water Line obtained from Villafáfila rainfall. The Evaporation Line for lake waters is indicated. B) Sulphate isotopic composition $\delta^{18}O_{SMOW}$ Vs $\delta^{34}S_{CDT}$ of lake and groundwaters in Villafáfila area. Relevant data for regional gypsum, mentioned in the text, are obtained from the literature, and have been plotted with smaller size for comparison. Huerta et al. (2010), Paleogene of the Almazán basin (dry mud flat and saline mud flat deposits); Utrilla et al. (1992), Late Triassic of the Iberian Chain and Miocene of the Madrid basin (Lower and Intermediate units); Alonso-Azcárate et al. (2006), Lower Cretaceous of the Cameros basin.

values, is interpreted as the low permeability Ordovician quartzites (Culebra Fm.) that crop out in the "Sierra de la Culebra", which constitutes the basement of the Cenozoic succession in this area. Background values for the basement in other areas of the Duero basin are about 30 Ohm/m (Nieto et al., 2020). The variable depths along profile 1 are in agreement with the existence of a palaeorelief below the Cenozoic succession of the Duero basin in its western margin (Martín Serrano and Piles Mateo, 1982). The tectonic structure of the metamophic rocks of the Sierra de la Culebra show WNW-ESE fold axes trends that continue below the Cenozoic succession towards the Villafáfila area, forming a basement elevation between the Salina Grande lake and Villarrín village. Outcrops of metamorphic rocks with the above-mentioned bedding orientation appear surrounded by Miocene rocks, 4 km W of the lakes (Fig. 2). The steep slope of GE-1 towards the SW of profile 1 could be interpreted as the occurrence of a high angle fault. GE-2 lies onto GE-1 and shows lower resistivities, but higher

Table 1
Radiocarbon dating of a water sample.

Sample data	pMC	$F^{14}C$	$\delta^{13}C$ ‰	$\delta^{18}O$ ‰	δD ‰
Beta - 570,623-P003 AMS-Standard delivery MATERIAL/PRETREATMENT: (water DIC) acidify-gas strip	1.24 +/− 0.04 pMC	0.0124 +/− 0.0004	−3.9	−9.85	−68.23

COMMENTS: The equivalent "Apparent" radiocarbon age to the reported pMC/fMDN values is ~35,280 BP (not adjusted for any hydro-geochemical effects on meteoric water 14CO2). Given the complex nature of groundwater DIC14 chemistry, duplicate measurements within 1–2 pMC are reasonable for a single water sample. For very low DIC concentration waters (< 20 mg/LHCO3) DIC14 and waters with complex organic chemistry, results can vary significantly outside of this expectation.

than in the overlying GE-3 unit. GE-2 is interpreted as the Salamanca Sandstone Formation or siderolithic unit (Corrochano, 1982; Santisteban et al., 1991) because of its stratigraphic position, its tabular geometry and its thickness. Salamanca Sandstone Fm. has siliceous cements, that reduce its porosity and permeability. GE-3 has low resistivities and is interpreted as the lower part of the Miocene aquifer (Martín Serrano and Piles Mateo, 1982), containing brackish (Type 3) groundwaters (TDS between 3200 and 5000 mg/L) observed in boreholes screened at depths below 40 m. Background resistivity values for the Miocene aquifer in the southern part of the Duero basin are about 20 Ohm/m (Nieto et al., 2020). Resistivities and position of GE-4 suggest that it corresponds with parts of the Miocene aquifer containing type 1 to type 2 waters, with salinities (TDS) ranging from 350 to 3500 mg/L. GE-4 in profile 2, below the hills (SEDT-7 station), corresponds with the shallow fresh groundwaters (Type 1), observed in dug wells. Towards the toe of the hills (SEDT-3 and 5) and below the lakes (SEDT-4) (Fig. 8B), GE-4 groundwaters become more saline (less resistive), which is consistent with the measured electric conductivities in mixed waters. In profile 1, GE-4 appears between GE-3 and 5 (Fig. 8A) and correlation of the two profiles, despite they do not actually cross each other, evidences the contribution of mixed groundwaters, coming from the hills and from deeper parts of the aquifer, to Salina Grande lake (Fig. 8B). Although profile 1 and 2 do not cross each other, SEDT-2 (profile 1) and SEDT-4 (profile 2) stations are 400 m apart. The top of GE-2 in SEDT-2 (profile 1) is at 600 masl, but in profile 2 has not been identified. This is interpreted as a consequence of the lateral geometry of the palaeorelief, that in SEDT-4 (profile 2) sinks the top of GE-2 to below 500 masl. The low resistivity of GE-5 corresponds with higher salinities of the brine (Type 3; TDS of 27,000 mg/L) contained in the Quaternary lake sediments aquitard. Profile 1 (Fig. 8A) shows that GE-5 sinks and its resistivity progressively decreases from Salina Grande lake towards the SW. This is interpreted as a flow pattern associated with the saline brine identified below the lakes and its progressive dilution. GE-6 shows high resistivity values and appears below the hills. It corresponds with the vadose zone and/or fresh groundwaters (type 1) observed in dug wells below the hills, tapping the upper parts of the Miocene aquifer.

5.2. Groundwater circulation in Villafáfila's lakes basin

Villafáfila area is poorly gauged, but a gross water balance has been made. The Villafáfila hydrological basin (156.5 km^2) balance for a steady state situation follows Eq. (1):

$$P + GWI = ETR + Ev + SR + GWO \quad (1)$$

Annual precipitation (P) represents 51.7 hm^3/yr (see Section 2.3). Deep groundwater input has been estimated with spring discharges at 0.75 hm^3/yr. Real evapotranspiration (ETR) is 36.3 hm^3/yr. Evaporation of lake's water (about 4 km^2 of pond areas) (Ev) is 2.9 hm^3/yr, and surface runoff (río Salado) 3.3 hm^3/yr (Fernández Pérez and Cabrera Lagunilla, 1987). Groundwater output (GWO) has been estimated by difference of terms as 10 hm^3/yr. This balance indicates the secondary role of groundwater inputs.

Hydrochemistry, hydraulic head and geophysics have revealed the occurrence of 1) local shallow fresh groundwater circulation, 2) regional deep brackish groundwaters and 3) a recycled lake brine.

1) Local fresh groundwaters (type 1) identified below the hills that surround the lakes have hydraulic heads about 720 to 710 masl. Water table depths range from about 7 m in dug wells located on the hills to decimetric depths at the toe of the hills. Despite the low number of data, mean isotopic values ($\delta D = -51.75‰$; $n = 2$; $\delta^{18}O = -7.08‰$; n = 2) of dug wells located on the hills are close to the LMWL (Fig. 7A) and are clearly different from those obtained from deep boreholes and springs. This suggests that fresh groundwaters identified in the hills are locally recharged and have not mixed with deep groundwaters. Horizontal gradients in the hills are typically 0.01–0.014 with a downward vertical component in the upper parts (Fig. 4B; S-002 and P-007). At the toe of the hills and in the lowlands surrounding the lakes the vertical component of groundwater flow is upwards. This is evidenced by the hydraulic head differences of boreholes opened at different depths, the occurrence of springs at the margins of Salina Grande and Barillos, and flowing artesian wells (depths >40 m) at the toe of the hills (Fig. 4). The groundwater specific discharges from the hills, considering the hydraulic conductivities for the Miocene aquifer, vary from 0.001 to 1 m/d. Geophysics (profile 2; Fig. 8B) evidences that these local fresh groundwaters lie onto more saline groundwaters that appear in the deeper parts of the Miocene aquifer (Fig. 8B). The contact between fresh groundwater lenses and the brackish deep groundwaters is about 100 m below the hills and becomes shallower at the hill toes (Fig. 8B). Towards the lakes these fresh-groundwaters (type 1) become more mineralized (type 2 and type 3) and appear sandwiched between brackish-saline groundwaters (Fig. 8B). Below appear brackish (TDS = 3200–5000 mg/L), deep groundwaters, identified in the lower parts of the Miocene aquifer. In the upper part, within the lake sediments aquitard, occurs a brine (TDS = 12,000–27,000 mg/L). This inversion of the salinity gradient is contrary to the density driven Ghyben-Herzberg relationship, which states that the less dense freshwater overlies the more dense saline groundwaters. This inverted salinity gradient can be explained by the low permeabilities of the lake aquitard and a continuous state of dynamic disequilibrium. In Lake Bonneville (Great basin) inverted salinity gradient has been attributed to the osmotic pressure effect (Mayo et al., 2020). In saline lakes like Fuente de Piedra (Kohfahl et al., 2008) or the Dead Sea (Yechieli and Wood, 2002) the depth of the saline - fresh water interface (Hs) is respectively 3.4 to 4.5 times the elevation of fresh groundwater (Hf) with respect to the playa lake level. In Villafáfila it is similarly about 3.3 (Fig. 8B).
2) Regional deep brackish (Type 3) groundwater appears mainly in springs surrounding Laguna Grande and in deep boreholes (depths >40 m). The TDEM survey has revealed its occurrence in the lower parts of the Miocene aquifer. Deep groundwaters are remarkably similar to each other, both when considering different locations and for different times of sampling of a single location. Physicochemical parameters are also quite constant (see Sections 4.2.1 and 4.2.2 above, and Table SM 2 - Suppl. Mat.) indicating that these waters have been thoroughly homogenized within the regional flow, likely pointing to large residence times (see Section 4.2.4). The average hydrogen and oxygen isotopic values ($\delta D = -70 \pm 2.8‰$; $n = 29$; $\delta^{18}O = -9.8 \pm 0.3‰$; $n = 26$) plot on the LMWL, but are lower, in absolute terms, than average local meteoric water ($\delta D = -51.5‰$; $\delta^{18}O = -7.2‰$), and close to precipitation occurring at the coldest months. This, together with the fact that deep groundwaters plot at values that are lower than the intersection between LMWL and the evaporation line (Fig. 7A) suggest that deep groundwaters are not

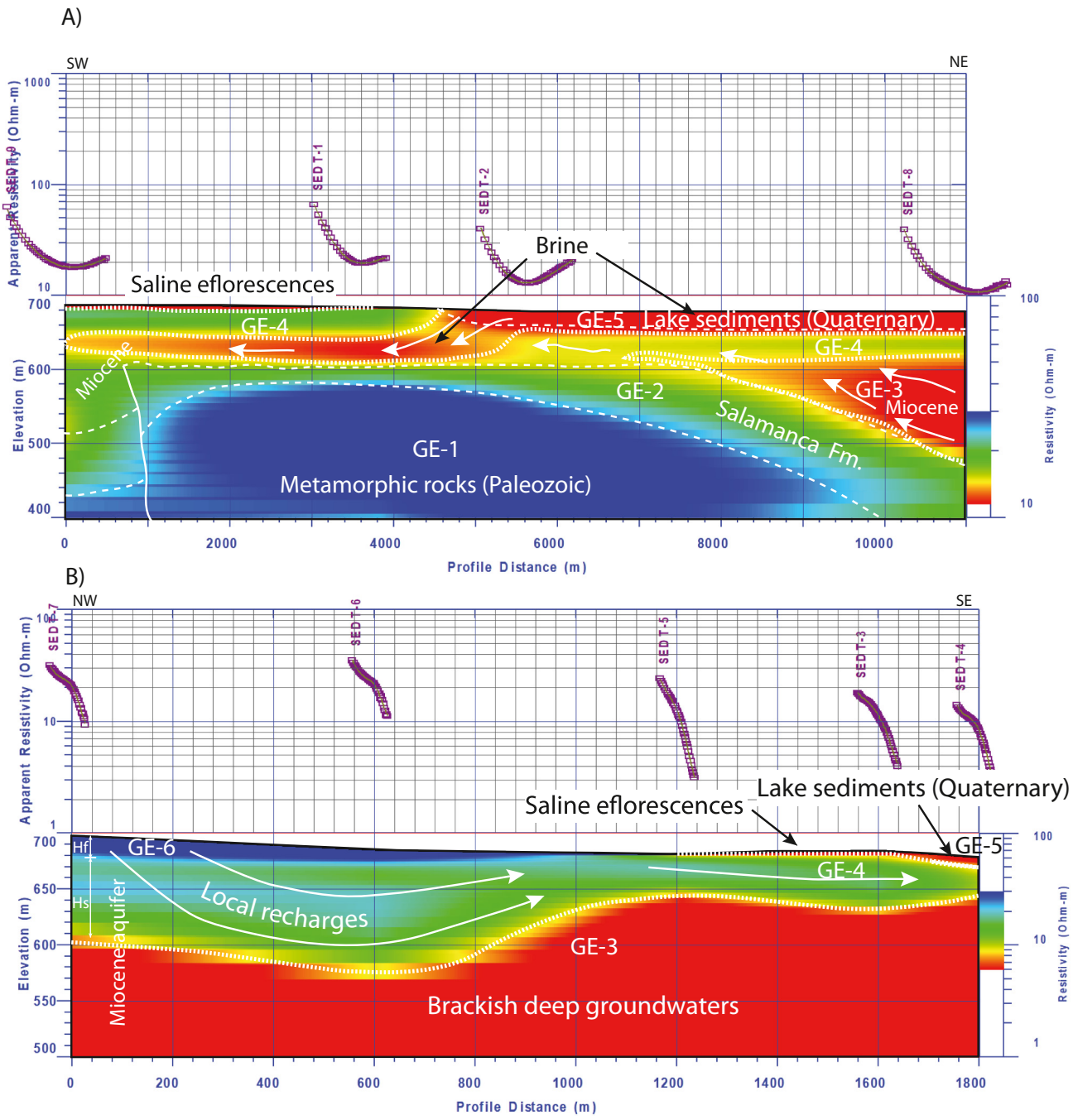

Fig. 8. Time Domain Electromagnetic profiles (TDEM), in Villafáfila (see location of stations in Fig. 2). A) Profile 1; B) Profile 2. GE are the geoelectric units. See text for description. Hs is the depth of the saline - fresh water interface. Hf is the elevation of fresh groundwater with respect to the lake level. Note that red colors indicate low resistivities (high salinities) and blue colors are high resistivities (low salinities). (For interpretation of the references to color in this figure legend, the reader is referred to the online version of this chapter.)

local precipitation. They probably represent precipitation occurring at lower average temperature that infiltrated into the aquifer, and travelled long distances before being tapped by deep boreholes or springs at the Villafáfila area. Considering regional water table map (Fig. 1), radiocarbon dating (20–30 Ky; see Section 4.2.4) and the average δD and $\delta^{18}O$ values, deep groundwaters infiltrated in moments (20–30 Ky ago) with climatic conditions cooler than current (Clark et al., 2009), and/or at high altitudes in the Cantabrian Mountains N and NE of Villafáfila.

3) Recycled high salinity brines (TDS = 12,000–27,000 mg/L) occur within the lake's sediment aquitard as have been observed in shallow piezometers (SGR-2 and SGR-3) (3.5 to 10 m deep) and in the TDEM profiles (Fig. 8). These highly mineralized brines are the product of the concentration by evaporation of lake waters during the summer, and by evaporation of groundwaters through the capillarity fringe when the lakes dry out, as it occurs in the Salar de Atacama (Kampf and Tyler, 2006; Marazuela et al., 2018). The shallow groundwater table below the lakes (0.6–0.9 m) at the end of the dry season supports the idea of evaporation by capillarity. Vertical gradients (0.14) measured at Salina Grande lake (Fig. 4C) would produce and ascendant groundwater specific discharge about 0.007–0.014 m/d during the summer, but it is compensated by evaporation via capillarity. During winter vertical gradients decrease when lake level is high. This brine was exploited to obtain salt through the excavation of holes from the Bronze age till the Middle age (Abarquero Moras et al., 2017). The lack of evaporite deposits on

the lake bottom is indicative of solute evacuation through groundwater output and the through-flow behavior of the Villafáfila lakes. This is in agreement with the southward flow of the brine, observed in TDEM profile 1, at the southwestern margin of Salina Grande (SEDT-2), when it abandons the aquitard constituted by the lake sediments and sinks towards the lower parts of the Miocene aquifer driven by its higher density (Fig. 8A). Salt efflorescences formed during the summer are dissolved with the first autumn rains and reincorporated into the brine.

5.3. Lake waters origin

Water balance of Villafáfila's lakes basin suggests that direct precipitation and local shallow groundwater are the main sources of water to the lakes, and despite the poor gauging of the lake levels, this is consistent with periodical observations (Fig. 3). Comparison of δD and $\delta^{18}O$ stable isotopes of rain, lake waters and groundwaters can be useful to understand how the different water sources contribute (Bocanegra et al., 2013; Cartwright et al., 2009; Valiente et al., 2019). Although precipitation samples only cover two consecutive meteorological years, the equation of the regression line through such data ($\delta D = 7.3\ \delta^{18}O + 2.1$) is very close to Craig's (1961) GMWL and can be used to define a local meteoric water line (LMWL) in the area, at least at the time of sampling. The validity of such LMWL is confirmed by comparison with the larger dataset (17 years of monthly samples, between January '2000 and December '2016; data obtained from the "Red de Vigilancia de Isótopos en Precipitación (REVIP)", managed by the "Centro de Estudios y Experimentación de Obras Públicas (CEDEX)" in collaboration with the "Agencia Estatal de Meteorología (AEMET)") from the meteorological stations at León (~80 kms N of Villafáfila; $\delta D = 7.47\ \delta^{18}O + 4.94$) and Valladolid (~75 kms ESE; $\delta D = 7.47\ \delta^{18}O + 3.70$). Isotopic mass balance, considering monthly precipitation at the sampling station (data from AEMET) results in average oxygen and hydrogen isotopic ratios of $\delta D = -51.5‰$ and $\delta^{18}O = -7.2‰$ for precipitation at Villafáfila during the sampled period.

δD and $\delta^{18}O$ in lake waters plot below the LMWL, and also show a good correlation ($\delta D = 5.2\ \delta^{18}O$ -14.1; $R^2 = 0.97$, for $n = 21$), defining an evaporation line whose slope is an indication of dominant relative humidity during evaporation. Keeping in mind that the slope of LMWL is less than 8, a slope of 5.2 for the evaporation line suggests average relative humidities around 70% (see Gonfiantini, 1986), which is within range of daily relative humidities measured at the Villafáfila Meteorological Station (data from AEMET). Extrapolation of the evaporation line to cut LMWL suggest values around $\delta D \approx -55‰$, $\delta^{18}O \approx -7.8‰$, which compare reasonably well with precipitation at Villafáfila during the sampled period (see above and Table SM 2 - Suppl. Mat.).

Despite precipitation is the main water contribution to the Villafáfila lakes, regional groundwater discharges are providing the solutes. Groundwater discharge to the lakes is evidenced by: a) the ascendant vertical component of the groundwater flow in the lake (vertical gradients of 0.15) and b) by the occurrence of brackish water springs in their surroundings with similar salinities and composition to those observed in deep boreholes (Type 3). Interpretation of TDEM profile 1 suggests the existence of upward groundwater flows with high salinities and long residence times (20–30 Ky) in the lower parts of the Miocene aquifer. This ascendant groundwater flow would be produced by the threshold resulting from elevation of the metamorphic basement from depths below 300 m to only 100 m at the SW of Salina Grande lake. Similar contributions occur in other through-flow or terminal lakes (Cartwright et al., 2009; Herczeg and Lyons, 1991; Tweed et al., 2009).

5.4. Solute sources

5.4.1. Shallow groundwaters in the hills

Low mineralization calcium-bicarbonate groundwaters, identified in the hills, obtained their composition from the dissolution of the carbonate cements and pedogenic nodules of the "Facies Tierra de Campos" unit that crops out in the hills surrounding the Villafáfila basin (Martín Serrano and Piles Mateo, 1982). The water table map of the Villafáfila hydrological basin points to a local groundwater flow from the hills towards the lakes (Fig. 4), suggesting that the Miocene rocks of the hills are the main contributor of solutes to the shallow groundwaters. $\delta^{18}O$ and δD values of shallow groundwaters in the hills are close to the average values of local rains, supporting the idea of local recharge and low evaporation.

5.4.2. Deep groundwaters

Na^+/Cl^- ratios of lake and groundwaters are close to 1, (Fig. 6) which is evidence of halite dissolution. On the other hand Ca^{2+}/SO_4^{2-} ratios are more variable, suggesting not only gypsum dissolution, but calcite or aragonite precipitation/dissolution processes as well. Na^+ Cl^- brackish groundwaters (Type 3) identified in boreholes (depths >40 m), and springs (Fig. 5) surrounding the lakes have obtained their solutes outside Villafáfila's lakes basin (Fernández Pérez and Cabrera Lagunilla, 1987). This is supported by the lack of known evaporites in the basin, but it is important to highlight that the nearest outcropping evaporites, in an upflow position, as indicated by regional water table map (Fig. 1) (CHD, 2009), are located about 150 km NE of Villafáfila. These evaporites are Triassic and Cretaceous in age and crop out in the Cantabrian Mountains (Cámara, 2017; Iribar and Ábalos, 2011). There are Cenozoic evaporites in the northeastern part of the Duero basin as well (Pineda Velasco, 1996; Siemcalsa, 1997), but not in the northern part (Herrero et al., 2004; Herrero et al., 2010), where the present-day groundwaters come from. As discussed before, deep groundwaters in Villafáfila correspond to regional discharges with long residence time in the aquifer system. The source of solutes could be far away from Villafáfila. Probably in the main recharge areas in the northern or northeastern part of the Duero aquifer system or in the Cantabrian Mountains. The following possible solute sources will be discussed below: 1) Triassic or Cretaceous evaporites in the Cantabrian Mountains; 2) Cenozoic evaporites in the Duero basin.

There is a great number of saline lakes in the Iberian Peninsula fed by groundwaters with solute sources located in Triassic evaporites (Jódar et al., 2020; Kohfahl et al., 2008; Luzón et al., 2007; Rodríguez-Rodríguez et al., 2006). Stable isotopes of water dissolved sulphate ($\delta^{34}S$; $\delta^{18}O$) are an important tool to identify possible solute sources specially when evaporites are involved (Iribar and Ábalos, 2011). Regional Triassic evaporites contain halite and gypsum and the isotopic signal of the gypsum can be identified in the dissolved sulphate. A wide isotopic data set is lacking for the Triassic gypsum of the Cantabrian Mountains, but values are well known for the Iberian Range (Alonso-Azcárate et al., 2006; Utrilla et al., 1992). Triassic gypsum from both the Cantabrian and Iberian ranges formed in coastal environments of the same basin (López-Gómez et al., 2002) and has isotopic values similar to those in other Alpine ranges (Longinelli and Flora, 2007). S and O isotopic ratios in sulphate from Villafáfila's lake waters and deep groundwaters range from $\delta^{34}S = +11.2$ to $+18.8‰$ and $\delta^{18}O = +10.8$ to $+17.8‰$ (with outliers mentioned removed). Average values for Triassic gypsum ($\delta^{34}S = +13.4 \pm 1.4‰$; $\delta^{18}O = +11.8 \pm 1.7‰$; (Utrilla et al., 1992) are similar to the lower values of the mentioned ranges (Table SM 2 - Suppl. Mat.; Fig. 7B). $\delta^{34}S$ values of Cenozoic gypsum from the Almazán basin (Colmenares section, dry mud flats; $\delta^{34}S = 11.8 \pm 0.6‰$;(Huerta et al., 2010) lie within the lower part of Villafáfila's $\delta^{34}S$ range. $\delta^{34}S$ values of Miocene gypsum from the Madrid basin (lower and intermediate units, $\delta^{34}S = 17.3 \pm 1.1‰$; (Utrilla et al., 1992), the Paleogene saline mudflats/ ephemeral lakes of the Almazán basin (Las Rozas and Monteagudo sections; $\delta^{34}S = 16.3 \pm 2.1‰$; (Huerta et al., 2010), and the Lower Cretaceous of the Cameros basin ($\delta^{34}S = 18.2 \pm 1.1‰$; (Alonso-Azcárate et al., 2006) -all formed under sulphate reducing conditions- lie within the upper part of Villafáfila's $\delta^{34}S$ range (Fig. 7B). Similarly, sulphur of Villafafila's dissolved sulphate could derive from waters that have dissolved Triassic

gypsum from the Cantabrian Mountains and maybe Cenozoic gypsums that precipitated from Triassic-derived sulphates in sulphate-reducing conditions. Obviously Almazán's, Madrid's and Cameros' basins gypsums have not contributed dissolved sulphate to Villafáfila's waters, due to their location and their different $\delta^{18}O$ values, but document processes that probably also affected the Cenozoic gypsums from the north-eastern part of the Duero basin. Although there are no sulphate isotopic data from the Cenozoic gypsum of the north-eastern part of the Duero basin, the playa-lakes "Facies Villatoro" and "Facies Bureba" units (Pineda Velasco, 1996) are similar to those described in the central Duero basin (Lower-Middle Miocene, $\delta^{34}S = 14.3 \pm 0.9‰$, 1σ, $n = 7$; Middle-Upper Miocene $\delta^{34}S = 15.7 \pm 0.6‰$, 1σ, $n = 34$; (Armenteros and Recio, 1995). If Cenozoic evaporites of the north-eastern part of the Duero basin were a solute source for deep groundwaters in Villafáfila, a change in the palaeogroundwater path lines is implied to explain the northeast-southwest flow trajectories.

5.4.3. Lake waters

Solutes in lake waters come mainly from deep groundwaters and the brine below the lakes, which show high TDS (Type 3), and a minor amount from shallow groundwaters recharged in the hills that are less mineralized. Evaporation of lake water concentrates the brine and a small amount of salts precipitate in the vadose zone. These salts are dissolved during the following rainy period and reincorporated to the brine. Some low Ca^{2+}/SO_4^{2-} and high Mg^{2+}/Ca^{2+} ratios (Fig. 6) in lake waters could be favored by calcite precipitation. Precipitated calcite is documented in lake-bottom sediments and cores (Cidón Trigo, 2016; Martín Bermudez, 2018; Santisteban et al., 2003). The occurrence of sulphate reduction processes in lake bottoms is supported by the high $\delta^{34}S$ of some lake water samples with values around +25‰.

6. Conclusions

Villafáfila lakes are through flow lakes located 40 km to the N of the Duero River. These lakes are ephemeral and only contain water during winter and spring (November–June). Most lake water comes from direct precipitation and shallow groundwaters but there are minor contributions from runoff and deep groundwaters as well.

Three types of water have been identified in the Villafáfila area according to groundwater chemistry. Type 1 are freshwaters with Ca^{2+}, HCO_3^- compositions that appear below the hills surrounding the lakes. Type 2 are mixed groundwaters dominated by HCO_3^-, Cl^- and Na^+ that appear at the toe of the hills. Type 3 are high salinity Na^+ Cl^- waters that can be identified in lake waters, in the springs surrounding the lake and in boreholes with depths >40 m. Type 1 represents local groundwater recharge in the hills. Type 2 corresponds with a mix of Type 1 and Type 3 waters at the toe of the hills. Type 3 corresponds with deep groundwaters with high residence time in the aquifer as evidenced by the lack of seasonal variations in their chemical and isotopic composition, and by their radiocarbon ages (22.3–28.9 ky). Regional water table map indicates that these deep groundwaters come from the NNE of the Duero basin and/or the Cantabrian Mountains.

TDEM survey, groundwater heads and the occurrence of flowing artesian wells (depths >40 m) with brackish waters have evidenced that deep groundwaters flow upwards due to the existence of a basement elevation that forces the deep groundwaters to rise. Underneath the lakes, and within the Quaternary lake sediments that behave as an aquitard, a saline brine reaching TDS = 27 g/L occurs. As observed in TDEM profile 1, a density inversion exists below the lakes where less saline mixed waters, like those identified at the toe of the hill, are sandwiched between the brackish deep groundwater and the saline brine. The brine flows towards the SW, abandoning the lake sediments aquitard and sinking towards deeper parts of the Miocene aquifer. This hinders the over-saturation with respect to halite in lake waters and in the brine.

Solutes (mainly Ca^{2+} and HCO_3^-) in the shallow groundwaters below the hills come from calcretes and carbonate nodules in the Miocene succession ("Tierra de Campos Unit"). The solutes from deep groundwaters come from the dissolution of Triassic and Cenozoic evaporites, mainly halite and gypsum, from the eastern part of the Cantabrian Mountains and the north-eastern part of the Cenozoic Duero basin.

This research has evidenced that shallow groundwaters below the hills in Villafáfila have low salinities till elevations about 600 masl and can be used for human consumption. In contrast, regional brackish groundwaters are the main source of solutes to the ecosystem of Villafáfila's Lakes Reserve. The data and conclusions of this paper could be useful for the environmental management of the Natural Reserve of the Villafáfila lakes and to compare the present situation with future scenarios. Villafáfila area is an excellent example to study the regional groundwater flow of the northern part of Duero hydrological basin. The origin of the lakes' salinity will be of interest for the archaeologist that study salt exploitation in western Iberia for the Bronze age - Middle age period.

Supplementary data to this article can be found online at https://doi.org/10.1016/j.scitotenv.2021.147909.

CRediT authorship contribution statement

Pedro Huerta: Investigation, Conceptualization, Writing – original draft. **Ildefonso Armenteros:** Investigation, Methodology, Writing – review & editing. **Clemente Recio:** Investigation, Methodology, Writing – review & editing. **Pedro Carrasco-García:** Investigation, Resources, Formal analysis. **Carolina Rueda-Gualdrón:** Data curation. **Azahara Cidón-Trigo:** Data curation.

Declaration of competing interest

The authors declare that they have no known competing financial interests or personal relationships that could have appeared to influence the work reported in this paper.

Acknowledgements

This research has been financially assisted by a grant from the Spanish "Ministerio de Ciencia, Innovación y Universidades" under research projects PGC2018-094566-B-C21 and CGL2014-54818-P. We want to thank the Consejería de Fomento y Medio Ambiente, Junta de Castilla y León, and the Casa del Parque (Villafáfila) for permission to do fieldwork in the Villafáfila lakes.

References

Abarquero Moras, F.J., Guerra Doce, E., Delibes de Castro, G., López Sáez, J.A., 2017. La explotación de la sal durante la Prehistoria en las Lagunas de Villafáfila (Zamora): Los cocederos de Molino Sanchón II y Santioste. Cuaternario y Geomorfologia 31 (1–2). https://doi.org/10.17735/cyg.v31i1-2.53646.

AEMET, 2020. AEMET open data. Benavente, http://www.aemet.es/es/datos_abiertos/AEMET_OpenData.

Al-Garni, M.A., El-Kaliouby, H.M., 2011. Delineation of saline groundwater and sea water intrusion zones using transient electromagnetic (TEM) method, Wadi Thuwal area, Saudi Arabia. Arab. J. Geosci. 4 (3–4), 655–668.

Alonso-Azcárate, J., Bottrell, S., Mas, J., 2006. Synsedimentary versus metamorphic control of S, O and Sr isotopic compositions in gypsum evaporites from the Cameros Basin, Spain. Chem. Geol. 234 (1), 46–57.

Alonso-Gavilán, G., Armenteros, I., Carballeira, J., Corrochano, A., Huerta, P., Rodríguez, J.M., 2004. Cuenca del Duero. In: Vera, J.A. (Ed.), Geología de España. SGE-IGME, Madrid, pp. 548–555.

Armenteros, I., Recio, C., 1995. Composición Isotópica de los yesos teciarios de la cuenca del Duero. Resultados preliminares. In: Melendez, A., Aurrel, M. (Eds.), XIII Congreso Español de Sedimentología, Teruel, pp. 139–140.

Armenteros, I., Corrochano, A., Alonso-Gavilán, G., Carballeira, J., Rodríguez, J.M., 2002. Duero basin (northern Spain). In: W. Gibbons, M.T. Moreno (Eds.), The Geology of Spain. The Geological Society, London, pp. 293–334.

Bahir, M., Ouazar, D., Ouhamdouch, S., 2018. Characterization of mechanisms and processes controlling groundwater salinization in coastal semi-arid area using

hydrochemical and isotopic investigations (Essaouira basin, Morocco). Environ. Sci. Pollut. Res. 25 (25), 24992–25004. https://doi.org/10.1007/s11356-018-2543-8.
Blanco, J.A., Armenteros, I., Huerta, P., 2008. Silcrete and alunite genesis in alluvial palaeosols (late Cretaceous to early Palaeocene, Duero basin, Spain). Sediment. Geol. 211 (1–2), 1–11.
Bocanegra, E., Londono, O.Q., Martinez, D.E., Romanelli, A., 2013. Quantification of the water balance and hydrogeological processes of groundwater–lake interactions in the Pampa Plain, Argentina. Environ. Earth Sci. 68 (8), 2347–2357.
Cámara, P., 2017. Salt and strike-slip tectonics as main drivers in the structural evolution of the Basque-Cantabrian Basin, Spain. In: Soto, J.I., Flinch, J.F., Tari, G. (Eds.), Permo-Triassic Salt Provinces of Europe, North Africa and the Atlantic Margins. Elsevier, pp. 371–393.
Cartwright, I., Weaver, T.R., Fulton, S., Nichol, C., Reid, M., Cheng, X., 2004. Hydrogeochemical and isotopic constraints on the origins of dryland salinity, Murray Basin, Victoria, Australia. Appl. Geochem. 19 (8), 1233–1254. https://doi.org/10.1016/j.apgeochem.2003.12.006.
Cartwright, I., Hall, S., Tweed, S., Leblanc, M., 2009. Geochemical and isotopic constraints on the interaction between saline lakes and groundwater in southeast Australia. Hydrogeol. J. 17 (8), 1991. https://doi.org/10.1007/s10040-009-0492-5.
CHD, 2009. Piezometría de Referencia (200 metros). http://www.mirame.chduero.es/.
Chebotarev, I.I., 1955. Metamorphism of natural waters in the crust of weathering–1. Geochim. Cosmochim. Acta, 8(1–2): 22–32, IN1-IN2, 33–48.
Cidón Trigo, A., 2016. Estudio sedimentológico y Geoquímico de las lagunas de Villafáfila a partir del análisis de dos tomas estacionales University of Salamanca, Salamanca, 39 pp.
Clark, P.U., Dyke, A.S., Shakun, J.D., Carlson, A.E., Clark, J., Wohlfarth, B., Mitrovica, J.X., Hostetler, S.W., McCabe, A.M., 2009. The last glacial maximum. Science 325 (5941), 710–714.
Coleman, M.L., Moore, M.P., 1978. Direct reduction of sulfates to sulfur dioxide for isotopic analysis. Analitical Chemistry 50 (11), 1594–1595.
Corrochano, A., 1982. El Paleógeno del borde occidental de la Cuenca del Duero (provincia de Zamora). Temas Geológicos Mineros, IGME 6 (2), 687–697.
Corrochano, A., Armenteros, I., 1989. Los sistemas lacustres de la Cuenca terciaria del Duero. Acta Geologica Hispanica 24 (3–4), 259–279.
Corrochano, A., Armenteros, I., Guerrero, O., Blanco, J.A., 2006. Arquitectura secuencial y paleoalteraciones en el dominio occidental de la cuenca terciaria del Duero. In: P. Huerta et al. (Eds.), Itinerarios Geológicos por la cuenca del Duero. Geo-Guías. Sociedad Geológica de España, Salamanca, pp. 43–71.
Craig, H., 1961. Isotopic variations in meteoric waters. Science 133 (3465), 1702–1703.
Cui, B.L., Li, X.Y., 2014. Characteristics of stable isotope and hydrochemistry of the groundwater around Qinghai Lake, NE Qinghai-Tibet Plateau, China. Environ. Earth Sci. 71 (3), 1159–1167. https://doi.org/10.1007/s12665-013-2520-y.
De la Hera-Portillo, A., López-Gutiérrez, J., Marín-Lechado, C., Martínez-Santos, P., Ruíz-Constán, A., Corral-Lledó, M.M., Galindo-Rodríguez, E., Mediavilla, R., Santisteban, J.I., Rodríguez-Jiménez, E., Callaú-Lópes, M.F., 2021. Integrating current and historical water chemistry data with long-term piezometric records to develop a regional-scale conceptual flow model: Las Salinas spring, Medina del Campo, Spain. Journal of Hydrology: Regional Studies, 34: 100781. doi:https://doi.org/10.1016/j.ejrh.2021.100781.
Donovan, J.J., Rose, A.W., 1994. Geochemical evolution of lacustrine brines from variable-scale groundwater circulation. J. Hydrol. 154 (1), 35–62. https://doi.org/10.1016/0022-1694(94)90211-9.
El-Kaliouby, H., 2020. Mapping sea water intrusion in coastal area using time-domain electromagnetic method with different loop dimensions. J. Appl. Geophys. 175, 103963.
Fernández Pérez, L., Cabrera Lagunilla, M.P., 1987. Estudio Hidrogeológico de las lagunas de Villafáfila (Zamora). Geología Ambiental y Ordenación del Territorio. III Reunión Nacional, Valencia, pp. 441–459.
Flores Avilés, G.P., Descloitres, M., Duwig, C., Rossier, Y., Spadini, L., Legchenko, A., Soruco, Á., Argollo, J., Pérez, M., Medinaceli, W., 2020. Insight into the Katari-Lago Menor Basin aquifer, Lake Titicaca-Bolivia, inferred from geophysical (TDEM), hydrogeological and geochemical data. J. S. Am. Earth Sci. 99. https://doi.org/10.1016/j.jsames.2019.102479.
Goldman, M., Gvirtzman, H., Hurwitz, S., 2004. Mapping saline groundwater beneath the Sea Galilee and its vicinity using time domain electromagnetic (TDEM) geophysical technique. Isr. J. Earth Sci. 53 (3–4), 187–197. https://doi.org/10.1560/P1W7-UYDE-WJFW-CVHB.
Gonfiantini, R., 1972. Notes on Isotope Hydrology, Internal Publication. IAEA Vienna.
Gonfiantini, R., 1986. Environmental isotopes in lake studies. In: Fritz, P., Fontes, J.C. (Eds.), Handbook of Environmental Isotope Geochemistry. Elsevier, Amsterdam, pp. 113–168.
González-Bernáldez, F., 1992. Ecological aspects of wetland/groundwater relationships in Spain. Limnetica 8, 11–26.
Han, L.F., Plummer, L.N., 2016. A review of single-sample-based models and other approaches for radiocarbon dating of dissolved inorganic carbon in groundwater. Earth Sci. Rev. 152, 119–142. https://doi.org/10.1016/j.earscirev.2015.11.004.
Hardie, L.A., Smoot, J.P., Eugster, H.P., 1978. Saline lakes and their deposits: A sedimentological approach. In: Matter, A., Tucker, M.E. (Eds.), Modern and Ancient Lake Sediments. International Association of Sedimentologists Special Publication, pp. 7–41.
Herczeg, A.L., Lyons, W.B., 1991. A chemical model for the evolution of Australian sodium chloride lake brines. Palaeogeogr. Palaeoclimatol. Palaeoecol. 84 (1–4), 43–53.
Herrero, A., Alonso-Gavilán, G., Colmenero, J.R., 2004. Estratigrafía del subsuelo en el sector noroeste de la Cuenca del Duero (Provincia de León). Rev. Soc. Geol. Esp. 17 (3–4), 199–216.
Herrero, A., Alonso-Gavilán, G., Colmenero, J.R., 2010. Depositional sequences in a foreland basin (north-western domain of the continental Duero basin, Spain). Sediment. Geol. 223 (3), 235–264. https://doi.org/10.1016/j.sedgeo.2009.11.012.
Huerta, P., Armenteros, I., Recio, C., Blanco, J.A., 2010. Palaeogroundwater evolution in playa–lake environments. Palaeogeogr. Palaeoclimatol. Palaeoecol. 286 (3–4), 135–148. https://doi.org/10.1016/j.palaeo.2009.12.008.
Huerta, P., Armenteros, I., Silva, P.G., 2011. Large-scale architecture in non-marine basins: the response to the interplay between accommodation space and sediment supply. Sedimentology 58 (7), 1716–1736.
IGME, 1980. Investigación hidrogeológica de la Cuenca del Duero: sistemas n° 8 y 12. IGME, Madrid, p. 75.
IGME-DGA, 2009. Apoyo a la caracterización adicional de las masas de agua subterránea en riesgo de no cumplir los objetivos medioambientales en 2015. Demarcación Hidrográfica del Duero. Masa de agua subterránea 31 Villafáfila, 84.
Ingerson, E., Pearson, F., 1964. Estimation of age and rate of motion of groundwater by the 14C-method. Recent Researches in the Fields of Atmosphere, Hydrosphere and Nuclear Geochemistry, pp. 263–283.
Iribar, V., Ábalos, B., 2011. The geochemical and isotopic record of evaporite recycling in spas and salterns of the Basque Cantabrian basin, Spain. Appl. Geochem. 26 (8), 1315–1329.
Jacobson, G., Arakel, A.V., Yijian, C., 1988. The central Australian groundwater discharge zone: evolution of associated calcrete and gypcrete deposits. Aust. J. Earth Sci. 35 (4), 549–565. https://doi.org/10.1080/08120098808729469.
Jódar, J., Rubio, F.M., Custodio, E., Martos-Rosillo, S., Pey, J., Herrera, C., Turu, V., Pérez-Bielsa, C., Ibarra, P., Lambán, L.J., 2020. Hydrogeochemical, isotopic and geophysical characterization of saline lake systems in semiarid regions: the Salada de Chiprana Lake, Northeastern Spain. Sci. Total Environ. 728, 138848. https://doi.org/10.1016/j.scitotenv.2020.138848.
Jones, B.F., Eugster, H.P., Rettig, S.L., 1977. Hydrochemistry of the Lake Magadi basin, Kenya. Geochim. Cosmochim. Acta 41 (1), 53–72. https://doi.org/10.1016/0016-7037(77)90186-7.
Jones, B.F., Naftz, D.L., Spencer, R.J., Oviatt, C.G., 2009. Geochemical evolution of Great Salt Lake, Utah, USA. Aquat. Geochem., 15(1): 95–121. https://doi.org/10.1007/s10498-008-9047-y.
Kampf, S.K., Tyler, S.W., 2006. Spatial characterization of land surface energy fluxes and uncertainty estimation at the Salar de Atacama, Northern Chile. Adv. Water Resour. 29 (2), 336–354.
Kohfahl, C., Rodriguez, M., Fenk, C., Menz, C., Benavente, J., Hubberten, H., Meyer, H., Paul, L., Knappe, A., López-Geta, J.A., Pekdeger, A., 2008. Characterising flow regime and interrelation between surface-water and ground-water in the Fuente de Piedra salt lake basin by means of stable isotopes, hydrogeochemical and hydraulic data. J. Hydrol. 351 (1), 170–187. https://doi.org/10.1016/j.jhydrol.2007.12.008.
Levi, E., Goldman, M., Hadad, A., Gvirtzman, H., 2008. Spatial delineation of groundwater salinity using deep time domain electromagnetic geophysical measurements: a feasibility study. Water Resour. Res. 44 (12). https://doi.org/10.1029/2007WR006459.
Longinelli, A., Flora, O., 2007. Isotopic composition of gypsum samples of Permian and Triassic age from the north-eastern Italian Alps: palaeoenvironmental implications. Chem. Geol. 245 (3), 275–284. https://doi.org/10.1016/j.chemgeo.2007.08.009.
López Sáez, J.A., Abel Schaad, D., Iriarte, E., Alba Sánchez, F., Pérez Díaz, S., Guerra Doce, E., Delibes de Castro, G., Abarquero Moras, F.J., 2017. Una perspectiva paleoambiental de la explotación de la sal en las Lagunas de Villafáfila (Tierra de Campos, Zamora). Cuaternario y Geomorfologia 31 (1–2), 31. https://doi.org/10.17735/cyg.v31i1-2.54255.
López-Gómez, J., Arche, A., Pérez-López, A., 2002. Permian and Triassic. In: W. Gibbons, T. Moreno (Eds.), The Geology of Spain. Geological Society of London, London, pp. 185–212.
Lusczynski, N.J., 1961. Head and flow of ground water of variable density. J. Geophys. Res. 66 (12), 4247–4256.
Luzón, A., Pérez, A., Sánchez, J.A., Soria, A.R., Mayayo, M.J., 2007. Evolution from a freshwater to saline lake: a climatic or hydrogeological change? The case of Gallocanta Lake (northeast Spain). Hydrol. Process. 21 (4), 461–469. https://doi.org/10.1002/hyp.6243.
Marazuela, M.A., Vázquez-Suñé, E., Custodio, E., Palma, T., García-Gil, A., Ayora, C., 2018. 3D mapping, hydrodynamics and modelling of the freshwater-brine mixing zone in salt flats similar to the Salar de Atacama (Chile). J. Hydrol. 561, 223–235. https://doi.org/10.1016/j.jhydrol.2018.04.010.
Martín Bermudez, I., 2018. Estudio sedimentológico y mineralógico de la sedimentación reciente en las lagunas de Villafáfila, University of Salamanca, Salamanca, 40 pp.
Martín Serrano, A., Barba Martín, A., 1979. Manganeses de la Lampreana 340, Mapa Geológico de España y Memoria. Escala 1:50.000. IGME, Madrid.
Martín Serrano, A., Piles Mateo, E., 1982. Villafáfila (308), Mapa Geológico de España y Memoria, Escala 1:15.000. IGME, Madrid.
Mayo, A.L., Tingey, D.G., Rey, K.A., Winkel, T.D., McBride, J.H., Nelson, S.T., Carling, G.T., Bruthans, J., Petersen, E.C., 2020. Shallow groundwater flow and inverted fresh/saline-water interface in a hypersaline endorheic basin (Great Basin, USA). Hydrogeol. J. 1–26.
Merritt, A.J., Chambers, J.E., Wilkinson, P.B., West, L.J., Murphy, W., Gunn, D., Uhlemann, S., 2016. Measurement and modelling of moisture–electrical resistivity relationship of fine-grained unsaturated soils and electrical anisotropy. J. Appl. Geophys. 124, 155–165. https://doi.org/10.1016/j.jappgeo.2015.11.005.
Mizutani, Y., Oana, S., 1973. Separation of CO2 from SO2 with frozen n-pentane as a technique for the precision analysis of 18O in sulfates. Journal of the Mass Spectrometry Society of Japan 21 (3), 255–258.
Navarro Alvargonzález, A., Fernández Uría, A., Doblas Domínguez, J.G., 1993. Las aguas subterráneas en España. ITGE, p. 600.

Nieto, I.M., Carrasco García, P., Sáez Blázquez, C., Farfán Martín, A., González-Aguilera, D., Carrasco García, J., 2020. Geophysical prospecting for geothermal resources in the south of the Duero Basin (Spain). Energies 13 (20), 5397.
Ouhamdouch, S., Bahir, M., Ouazar, D., Carreira, P.M., Zouari, K., 2019. Evaluation of climate change impact on groundwater from semi-arid environment (Essaouira Basin, Morocco) using integrated approaches. Environ. Earth Sci. 78 (15), 449. https://doi.org/10.1007/s12665-019-8470-2.
Parkhurst, D.L., Appelo, C., 2013. Description of input and examples for PHREEQC version 3: A computer program for speciation, batch-reaction, one-dimensional transport, and inverse geochemical calculations. 2328–7055, US Geological Survey.
Pearson Jr., F., White, D., 1967. Carbon 14 ages and flow rates of water in Carrizo Sand, Atascosa County, Texas. Water Resour. Res. 3 (1), 251–261.
Pedrera, A., Martos-Rosillo, S., Galindo-Zaldívar, J., Rodríguez-Rodríguez, M., Benavente, J., Martín-Rodríguez, J., Zúñiga-López, M., 2016. Unravelling aquifer-wetland interaction using CSAMT and gravity methods: the Mollina-Camorra aquifer and the Fuente de Piedra playa-lake, southern Spain. J. Appl. Geophys. 129, 17–27.
Pineda Velasco, A., 1996. El enlace y la paleogeografía neógena entre las Cuencas del Duero y el Ebro en La Bureba (Burgos). Boletin Geológico y Minero 107, 14–28.
Rafter, T., 1967. Oxygen isotopic composition of sulphates part 1, a method for the extraction of oxygen and its quantitative conversion to carbon dioxide for the isotope ratio measurements. New Zealand Jour. Sci. 10, 493–510.
Robinson, B.W., Gunatilaka, A., 1991. Stable isotope studies and the hydrological regime of sabkhas in southern Kuwait, Arabian Gulf. Sediment. Geol. 73 (1), 141–159. https://doi.org/10.1016/0037-0738(91)90027-B.
Robinson, B.W., Kusakabe, M., 1975. Quantitative preparation of sulfur dioxide for $^{34}S/^{32}S$ analyses from sulfides by combustion with cuprous oxide. Analitical Chemistry 47 (7), 1179–1181.
Rodríguez-Rodríguez, M., Benavente, J., Cruz-San Julián, J.J., Moral Martos, F., 2006. Estimation of ground-water exchange with semi-arid playa lakes (Antequera region, southern Spain). J. Arid Environ. 66 (2), 272–289. https://doi.org/10.1016/j.jaridenv.2005.10.018.
Ruiz-Constán, A., Pedrera, A., Martos-Rosillo, S., Galindo-Zaldívar, J., Martín-Montañés, C., González de Aguilar, J.P., 2015. Structure of a complex carbonate aquifer by magnetic, gravity and TDEM prospecting in the Jaén area, southern Spain. Geol. Acta 13 (3), 191–203.
Saeed, W., Shouakar-Stash, O., Unger, A., Wood, W.W., Parker, B., 2021. Origin of solutes in a regional multi-layered sedimentary aquifer system (a case study from the Rub' al Khali basin, Saudi Arabia). Applied Geochemistry 126. https://doi.org/10.1016/j.apgeochem.2021.104871.
Sakai, H., Krouse, H., 1971. Elimination of memory effects in 18O/16O determinations in sulphates. Earth Planet. Sci. Lett. 11 (1–5), 369–373.
Salem, O., Visser, J., Dray, M., Gonfiantini, R., 1980. Groundwater Flow Patterns in the Western Libyan Arab Jamahiriya Evaluated from Isotopic Data, Arid-Zone Hydrology: Investigations with Isotope Techniques. IAEA, Vienna, pp. 165–179.
Santisteban, J.I., Mediavilla, R., Martín Serrano, A., 1991. El Paleógeno del sector suroccidental de la Cuenca del Duero: nueva división estratigráfica y controles sobre su sedimentación. Acta Geologica Hispanica 26 (2), 133–148.
Santisteban, J.I., García del Cura, M.A., Mediavilla López, R., Dabrio, C.J., 2003. Estudio preliminar de los sedimentos recientes de las Lagunas de Villafáfila (Zamora). Geogaceta 33, 51–54.
Siemcalsa, 1997. Mapa Geológico y Minero de Castilla y León Escala 1:400.000. Junta de Castilla y León, Valladolid.
Tchouta, K.D., Marie, B., Emmanuel, M.V.Y., Guillaume, F., Benjamin, N.N., Nicaise, Y., Baba, G.I., Anatoly, L., 2019. Contribution of time domain electromagnetic and magnetic resonance soundings to groundwater assessment at the margin of Lake Chad Basin, Cameroon. J. Appl. Geophys. 170, 103840. https://doi.org/10.1016/j.jappgeo.2019.103840.
Thornthwaite, C.W., Mather, J.R., 1955. The Water Balance Publications in Climatology. Drexel Institute of Climatology, Centerton, New Jersey, pp. 1–104.
Tweed, S., Leblanc, M., Cartwright, I., 2009. Groundwater–surface water interaction and the impact of a multi-year drought on lakes conditions in South-East Australia. J. Hydrol. 379 (1), 41–53. https://doi.org/10.1016/j.jhydrol.2009.09.043.
Utrilla, R., Pierre, C., Ortí, F., Pueyo, J.J., 1992. Oxygen and sulphur isotope compositions as indicators of the origin of Mesozoic and Cenozoic evaporites from Spain. Chem. Geol. 102, 229–244.
Valiente, N., Sanz, D., Gómez-Alday, J.J., 2019. Groundwater recharge by high-salinity lake water in a density-driven flow dominated system: an isotopic approach, E3S Web of Conferences. EDP Sciences, pp. 12024.
Wassenaar, L.I., Athanasopoulos, P., Hendry, M.J., 2011. Isotope hydrology of precipitation, surface and ground waters in the Okanagan Valley, British Columbia, Canada. J. Hydrol. 411 (1), 37–48. https://doi.org/10.1016/j.jhydrol.2011.09.032.
Waxman, M.H., Smits, L.J.M., 1968. Electrical conductivities in oil-bearing shaly sands. Soc. Pet. Eng. J. 8 (02), 107–122. https://doi.org/10.2118/1863-A.
Yechieli, Y., Wood, W.W., 2002. Hydrogeologic processes in saline systems: playas, sabkhas, and saline lakes. Earth Sci. Rev. 58 (3), 343–365. https://doi.org/10.1016/S0012-8252(02)00067-3.
Young, M., De Bruijn, R., Al-Ismaily, A.S., 1998. Exploration of an alluvial aquifer in Oman by time-domain electromagnetic sounding. Hydrogeol. J. 6 (3), 383–393.